Contents

Model intercomparison study for cadmium

About EMEP/MSC-E participation in ATMES-II

Model intercomparison studies for cadmium

Alexey Gusev, Ilia Ilyin, Gerhard Petersen, Addo van Pul, Dimiter Syrakov

Introduction

This report presents description of the results of cadmium model intercomparison study. It comprises the description of intercomparison procedure, methodology, input data and participated models.

Model intercomparison studies are an important stage in the development of models. The intercomparison of transport models for heavy metals (HM) was initiated by recommendations of the EMEP workshop held in Beekbergen in 1994 and the 18th session of the EMEP Steering Body. This study was aimed at the comparison of approaches used for evaluating of HM transport and deposition within the scope of European region. Beginning with the lead model intercomparison in 1996, this activity has been continued with cadmium study and is planned to be continued for mercury models. These intercomparisons form a sequence of studies which makes a valuable contribution to the development of modelling basis for HMs.

The intercomparison program for the first stage devoted to lead models was developed by a group of experts in the field of HM modelling representing DNMI (Norway), IVL (Sweden), RIVM (the Netherlands), IIASA (Austria), NILU (Norway), GKSS (Germany). MSC-E in collaboration with advisory expert group prepared a protocol, program and initial data for calculations. Seven regional lead models participated at the first stage. The comparison results were presented in the report submitted to the EMEP Steering Body [*EMEP/MSC-E report* 2/96, 1996].

The comparison of cadmium transport models for European region is the next stage of this activity. The group of experts from different scientific organizations, shown in Table 1, in cooperation with MSC-E has developed the program of the cadmium model intercomparison.

Table 1. Advisory expert group members

Experts	Organizations
Dr. J. Bartnicki	DNMI, Norway
Dr. A. Iverfeld	IVL, Sweden
Prof. J. Munthe	IVL, Sweden
Prof. J. Pacyna	NILU, Norway
Prof. G. Petersen	GKSS, Germany
Dr. A. van Pul	RIVM, the Netherlands
Prof. D. Syrakov	NIMH, Bulgaria

In view of the fact that actually the same models took part in this intercomparison study compared to previous one, a general approach was kept but the methodology was modified.

Cadmium in the environment

A number of investigations demonstrated that cadmium is toxic. It can be accumulated in tissues of plants and animals and enter the human organism with food, water and via respiratory organs. The intoxication by cadmium is as a rule of a cumulative character and it increases with age. For this reason increase of cadmium emissions to the atmosphere and therefore the elevation of its content in air and depositions is of a serious concern.

As a result of long-term scientific and political activity 36 countries Parties to the Convention signed new Protocol on Heavy Metals.

Cadmium is emitted to the atmosphere both by natural and anthropogenic sources. Natural sources can be volcanic activity, natural forest fires, wind erosion, meteor matter, the World Ocean. The intensity of natural sources is rather variable in time and space, therefore it is difficult to make quantitative assessment of natural emission. For this reason they can be rather scattered. *J.Nriagu* [1989] estimated that mean global cadmium input to the atmosphere is 1.3 kt/yr mainly due to volcanic activity (0.82 kt/yr).

Anthropogenic emission of cadmium is mainly conditioned by industrial activity. The main sources can be divided into following groups [*Skotnikova and Smirnova*, 1995]. The first one - iron and steel production, non-ferrous metallurgy, organic fuel combustion, building materials production (cement, glass, ceramics). The second group includes electric metallization, production of accumulators, pigments, and plastics. Waste incineration is referred to a separate group.

According to estimates of *J.Nriagu and J.Pacyna* [1989] global emission of cadmium for 1983 is 7.6 kt/yr (median value) ranging from 3.1 to 12.0 kt/yr.

As a rule, cadmium and its species are emitted to the atmosphere on aerosol particles. Particle sizes with regard to the type of sources can vary from 0.01 to 100 μm [*Ryaboshapko and Bryukhanov*, 1993]. Coarse particles are rapidly deposited near their sources, while intermediate and fine fractions can remain in the atmosphere for longer periods up to several days. Therefore particles of this size can be transported for a long distances from their sources being subject to transboundary or even transcontinental transport.

Two main mechanisms of Cd (particle bound) removal from the atmosphere are wet and dry deposition. Wet deposition is influenced by the type and intensity of precipitation. Dry deposition depends on several factors such as particle size, meteorological conditions and properties of underlying surface.

Cadmium airborne transport

For evaluation of Cd transport in the atmosphere a number of models have been developed in Europe. They can be divided into two large groups - models of Eulerian and Lagrangian types. In the first group the transport is calculated in the fixed co-ordinate system strictly linked with geographical grid. In the second group the co-ordinate system is connected with an air particle moving in the air flux. Each type of models has its advantages and shortcomings.

The models implement different description of vertical mixing and horizontal diffusion. Besides, independent of the type, each model uses different approaches for the description of wet and dry depositions as well as different parameterization of particle-carrier sizes.

Four regional models estimating the spatial distribution of cadmium concentrations and depositions over European region took part in the intercomparison. Table 2 presents the list of the models, their type and resolution. Their detailed descriptions can be found in the Annex B to this report.

Table 2. List of the models participating in the intercomparison

Model	Institute	Resolution	Model type
ASIMD (modified version)	MSC-E (Meteorological Synthesizing Centre – East) of EMEP	50×50 km^2	3D Eulerian
EMAP	National Institute of Meteorology and Hydrology, Bulgaria	50×50 km^2	3D Eulerian
GKSS	GKSS Research Centre, Geesthacht, Germany	150×150 km^2	2D Lagrangian
TREND	RIVM (Rijksinstituut Volksgezondheid en Milieu), Bilthoven, The Netherlands	50×50 km^2	2D Lagrangian

As seen from the Table 2, the models participated in the intercomparison are of different types. Two of them (GKSS, TREND) are two-dimensional Lagrangian models, other two (ASIMD, EMAP) - three-dimensional Eulerian models. Three of them (ASIMD, EMAP, TREND) use 50×50 km^2 horizontal resolution and GKSS uses 150×150 km^2 resolution.

Comparison procedure

There is a good experience gained in a number of projects aimed at the intercomparison of various models from numerical weather forecast models to airborne pollution transport models of local, regional and global scale. The main objective of a given intercomparison, as well as of the previous one for lead, was the comparison of approaches used for HM transport modelling by different groups of scientists. The answer to the question - how close are modelling results - is of particular interest. The lack of measurement data and a considerable uncertainty of HM emissions do not allow to use sophisticated methods of comparison and analysis of calculation results at this stage.

The suggested methodology is similar to those used in other projects on the comparison, for example, ETEX [*Graziani et al.*, 1998]. It should be noted that in distinction from ETEX project, in which the transport of a neutral pollutant was considered during a short episode, this study deals with transport of trace metal, cadmium, and calculations are made within the EMEP region for the whole year (1990). The comparison of model results with measurements makes the basis for the study. As at the previous stage for lead intercomparison procedure involves calculations of transboundary transport on example of three countries – Italy, Poland and United Kingdom.

Emission data

In the recent years several estimates of cadmium emissions in Europe were made for different years [*Axenfeld et al.*, 1992; *Pacyna et al.*, 1995; *van den Hout*, 1994; *Berdowski et al.*, 1997]. Most of them are referred to the late 1980-s and 1990. As at the previous stage for lead expert estimates of Cd emission of ESQUAD project were chosen. The overall uncertainty of these data was estimated to be within the range of a factor of ±2.5 - 3. With respect to the range of uncertainty of emission factors used there were three sets of emission estimates - low, average, and high. According to the recommendations of the emission experts high values of ESQUAD project Cd emissions for 1990 were used in calculations. UBA emission estimates for 1990 were not available in electronic form at the moment of the model comparison.

For modelling cadmium emission was presented on the EMEP grid with spatial resolution 150×150 km^2 and 50×50 km^2. Temporal variations were not considered. It was assumed that emissions are uniform round the year. Each model determined emission distribution with height separately.

Figure 1 presents the spatial distribution of emission data used for modelling. National totals of Cd emission of European countries for 1990 according to ESQUAD project are given in Table 3.

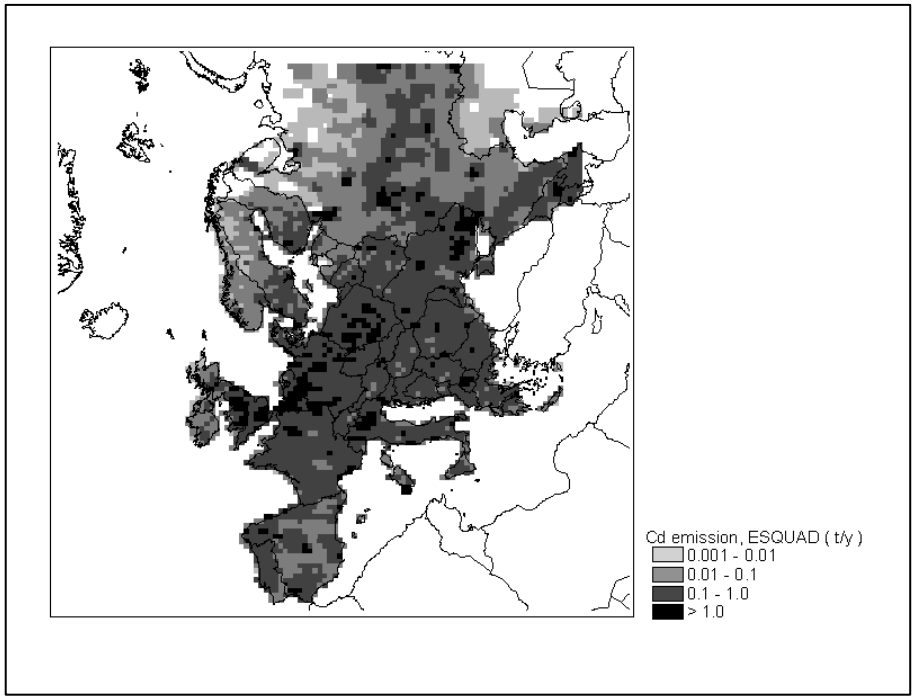

Figure 1. Cd emissions for 1990 according to ESQUAD project estimates

Table 3. Cd emission data for European countries according to ESQUAD project. Units: t/yr

Country	Estimates for 1990 [van den Hout(ed.), 1994] ESQUAD		
	Low	Average	High*
Albania	0	1	4
Austria	2	4	9
Belgium	5	18	40
Bulgaria	2	8	24
Former Czechoslovakia	4	18	32
Denmark	1	2	6
Finland	2	5	23
France	23	46	101
Germany	37	74	204
Greece	2	5	16
Hungary	2	5	9
Iceland	0	0	0
Ireland	1	1	3
Italy	**18**	**48**	**141**
Luxembourg	0	1	2
Netherlands	3	5	10
Norway	1	2	5
Poland	**21**	**46**	**132**
Portugal	1	3	12
Romania	4	16	38
Spain	8	21	70
Sweden	4	8	31
Switzerland	2	4	7
United Kingdom	**26**	**52**	**121**
Former USSR[1)]	66	167	517
Former Yugoslavia	8	23	68
Total	**242**	**584**	**1634**

* data used in calculations

1) within the EMEP grid

Measurement data

In accordance with intercomparison procedure mean annual concentrations of cadmium in air and precipitation and wet deposition were used in the model intercomparison. For this purpose measured concentrations of cadmium in Europe for 1990 were selected. Such measurements were carried out within the framework of international programmes HELCOM, OSPARCOM, EMEP. At present due to the co-operation between these programmes measurement data are being accumulated in the database of CCC of EMEP.

The list of stations which measurement results were used is given in Table A1. Measurements of Cd air concentrations at 17 stations, and Cd concentrations in precipitation at 31 stations for 1990 are available. The location of stations within the EMEP region is shown on Figure 2. As seen from the figure the majority of stations are located in the north-western part of the region.

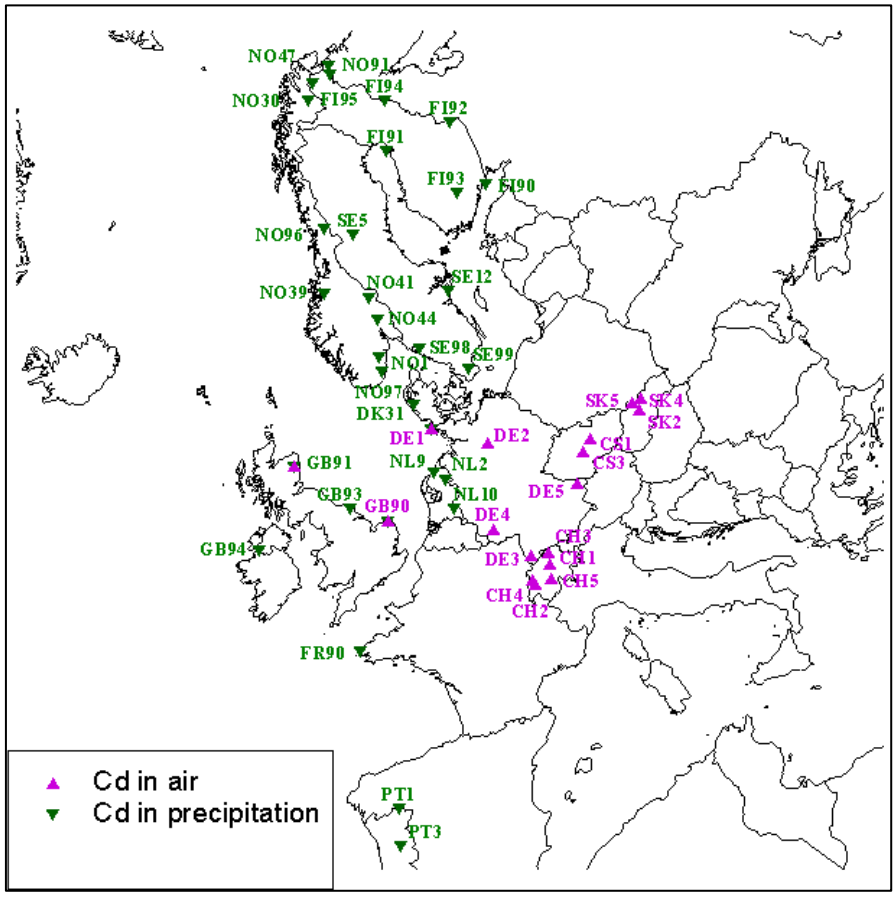

Figure 2. Location of stations with available Cd measurements for 1990

Some measurement data were excluded for the following reasons (these values are given in italic in Table A1).

Data of stations NO96 and NO97 are incomplete for the whole 1990 (measurements were made only for four months of 1990).

Data of stations GB94, PT1, PT3 were excluded according to the recommendation of CCC of EMEP.

Data of station CH1 were excluded because this station is located at 3.5 km height. This height is outside the calculation domain of some models.

Selected data set has some disadvantages. The south-eastern part of the EMEP region is not covered by measurements. Only three stations provided parallel measurements of cadmium concentrations in air and precipitation. Observations of the Finnish stations, in particular, of FI92, FI93, FI94, FI95, were made not for the whole year 1990 (see table A1). Therefore their data sets are incomplete. The information on representativeness of stations is not available.

Meteorological data

In accordance with intercomparison procedure participated models used meteorological data for 1990. The use of meteorological data is closely connected with the model structure, therefore each model utilized its own meteorological data set. ASIMD and EMAP used 6-hour instantaneous meteorological fields obtained from Russian Hydrometeorological Centre. TREND model used long-term averages obtained from Dutch meteorological office. GKSS model used 6-hour instantaneous meteorological fields obtained from Norwegian Numerical Weather Prediction Model and from the European monitoring network.

Comparison with measurements

Calculated and measured values of mean annual cadmium concentrations in air and precipitation and wet deposition for 1990 were compared. To quantitatively compare modelling results the following statistical parameters often used in other procedures [*Hanna*, 1988; *Graziani et al.*, 1998] were calculated:

- Fractional Bias – *FB*
- Fractional Standard Deviation – *FSD*
- Normalized Mean Square Error – *NMSE*
- Correlation Coefficient – *R*
- "Factor of 2" parameter – *FA*2

For calculation of statistical parameters the set of N pairs $\{(O_i, P_i)\}$ were used. $\{O_i\}$ and $\{P_i\}$ indicate the set of observations and the set of predictions, made by each model. $\overline{P}$ and $\overline{O}$ are the arithmetic means and σ_p and σ_o are the standard deviations of P and O.

Fractional Bias

$$FB = 2 \cdot \frac{\overline{P} - \overline{O}}{\overline{P} + \overline{O}} \tag{1}$$

Fractional Bias allows evaluating the bias of modelling results with regard to measurements or, in other words, the tendency to overestimation or underestimation of measurements. In the ideal case *FB* should be equal to zero.

Fractional Standard Deviation

$$FSD = 2 \cdot \frac{\sigma_P^2 - \sigma_O^2}{\sigma_P^2 + \sigma_O^2} \tag{2}$$

Fractional Standard Deviation makes it possible to evaluate how a model estimates the spread of measurements, i.e. it overestimates or underestimates scattering of measurement data.

Normalized Mean Square Error

$$NMSE = \frac{1}{N \cdot \overline{O} \cdot \overline{P}} \cdot \sum_i (O_i - P_i)^2 \tag{3}$$

Normalized Mean Square Error defines the agreement between calculated and measured values. The closer *NMSE* is to zero the better is correlation between calculated and measured data.

Correlation Coefficient

$$R = \frac{\sum_i (O_i - \overline{O}) \cdot (P_i - \overline{P})}{\sqrt{\sum_i (O_i - \overline{O})^2 \cdot \sum_i (P_i - \overline{P})^2}} \tag{4}$$

is a measure of linear dependence of calculated and measured values.

"Factor of 2" parameter

"Factor of 2" determines the fraction of calculated values within a factor of 2 compared with measurements.

In addition to statistical parameters regression coefficients were calculated and scatter plots were drawn.

These values indicate to what extent better or worse every participated model reproduces measured concentrations and depositions in comparison with other models. In general these parameters allow evaluating the tendency to overestimation/underestimation and the consistency with measured values.

Assessment of cadmium transboundary transport

Next stage of the intercomparison was devoted to the assessment of transboundary transport for three EMEP countries - Italy, Poland and United Kingdom. On the basis of calculations for each of three countries their contribution to the depositions on other EMEP countries and the fraction of total depositions from external sources were estimated. The calculation results show how each model assesses cadmium transboundary transport within the EMEP region.

The contribution of country sources to deposition on other countries

$$Export = \frac{E - OD}{E} \cdot 100\% \qquad (5)$$

The contribution to deposition on a country from other countries

$$\text{Import} = \frac{TD - OD}{TD} \cdot 100\% \qquad (6)$$

where: *TD* - total cadmium deposition on a country;

OD - cadmium deposition on a country from its own sources;

E - country emission.

Description of intercomparison results

At the first stage as it was envisaged by the procedure the calculation results of four models were compared with available measurements. In the comparison mean annual concentrations of cadmium in air and precipitation and wet deposition for 1990 were considered. The second stage involved the evaluation of cadmium transboundary transport. Below detailed results of the comparison with measurements will be considered. Additional information can also be found in Annexes to this report. Annex A contains scatter plots and tables with detailed results of the comparison with measurements. Annex C contains maps of deposition and concentrations for each participated model.

Air concentrations

Calculated mean annual concentrations of cadmium in the surface air were compared with observations of 16 stations. Mean observed Cd air concentration is 0.57 ng/m^3. The statistical parameters calculated on the basis of these data are presented in Table 4. Scatter plots of calculated and measured air concentrations are presented on Figure A1.

Table 4. Cd air concentrations, ng/m^3. Mean observed concentration is 0.57 ng/m^3

	ASIMD	EMAP	GKSS	TREND
Mean	**0.56**	0.76	0.53	0.91
FB	**-0.02**	0.29	-0.07	0.46
FSD	-1.13	**-0.16**	-1.22	-0.30
Correlation	0.28	0.25	**0.46**	0.34
FAC2	69%	69%	**88%**	56%
Slope	0.72	**1.00**	0.71	1.19
NMSE	0.45	0.55	**0.39**	0.55

As follows from the Table 4 the ASIMD model provides the best agreement (among the models considered here) with the mean observed value and consequently has the least bias.

The EMAP model is the most good in assessing measurement data scattering and its regression line slope is 1.

The GKSS model has the highest correlation coefficient and the least mean square error. For this model the biggest number of calculated values are within a factor of 2 with observations.

The results of TREND and GKSS models better correlates with observations in comparison with other two models.

The results of ASIMD and GKSS models tend to underestimate observations by about 30%. The EMAP model shows no deviation and TREND overestimates observed concentrations in air by about 20%.

Thus the systematic differences between the modelled air concentrations by the participated models are typically -30% - 20%.

Concentrations in precipitation

Mean annual concentrations of cadmium in precipitation were compared with observations of 26 stations. Mean observed concentration is 0.13 μg/l. The statistical parameters calculated for each model are presented in Table 5. Scatter plots of calculated and measured concentrations in precipitation are shown on Figure A2.

Table 5. Cd concentration in precipitation. Mean observed concentration is 0.13 μg/l

	ASIMD	EMAP	TREND
Mean	0.074	**0.086**	0.078
FB	-0.55	**-0.41**	-0.49
FSD	0.57	0.60	**0.15**
Correlation	0.48	0.46	**0.52**
FAC2	27%	**50%**	**50%**
Slope	0.59	**0.65**	0.59
NMSE	1.54	1.30	**1.04**

As evident from the Table 5 the results of EMAP model are closer to measurements than other models. This model has the least bias and its slope of regression line is closest to 1.

The TREND model demonstrates the highest correlation coefficient and the best estimate of measurement data scattering. It also has the biggest number of calculated values within a factor of 2 with observations.

For EMAP and TREND models 50% of calculated values are within a factor of 2 with observations. The EMAP, ASIMD and TREND models tend to underestimate measurements by 35%, 41% and 41% respectively.

Wet deposition

Calculated wet depositions of Cd were compared with observations of 26 stations. Mean observed wet deposition is 82.55 $\mu g/m^2$. Statistical parameters calculated on the basis of these data for each model are presented in Table 6. Scatter plots of calculated and measured concentrations in precipitation are shown on Figure A3.

Table 6. Cd wet deposition. Mean observed wet deposition is 82.55 μg/m^2

	ASIMD	EMAP	GKSS	TREND
Mean	**81.04**	88.11	77.21	54.26
FB	**-0.02**	0.07	-0.07	-0.41
FSD	1.26	1.22	0.74	**0.12**
Correlation	0.44	0.43	0.44	**0.51**
FAC2	**54%**	**54%**	46%	**54%**
Slope	0.96	**1.00**	0.82	0.61
NMSE	2.29	1.98	1.28	**1.18**

As seen from the Table 6 the ASIMD model has high correlation coefficient and the least bias. As to mean values its results are in a good agreement with measurements.

The EMAP has in this case the best slope of regression line equal to 1.

The TREND model has the best estimate of measurement data scattering, the lowest mean square error and also the highest correlation coefficient.

For EMAP, ASIMD and TREND 54% of calculated values are within a factor of 2 with observations. For GKSS model this parameter value is somewhat lower.

The EMAP model shows no systematic deviation from observed Cd wet depositions. ASIMD, GKSS and TREND tend to underestimate measurement data by 4%, 18% and 39%, respectively.

Precipitation amount

In addition to the comparison of concentrations and depositions annual precipitation amount measured and used in calculations were also compared. Data on precipitation amount were taken from the same 26 stations at which measurements of concentrations in precipitation were carried out. Correlation coefficients calculated for each model on the basis of these data are shown in Table 7. Mean observed value was 644 mm/yr.

Table 7. Comparison of precipitation amount. Mean observed value is 644 mm/yr

	ASIMD	EMAP	TREND
Mean precipitation amount	1024	981	**705**
Correlation	0.83	**0.85**	0.71

Although this value does not characterize model properties but meteorological data, it affects significantly model results and practically determining the obtained wet depositions and

correspondingly concentrations in precipitation and indirectly in air as well. As seen from Table 7 mean precipitation amount most close to measurements was used in the TREND model. At the same time higher correlation coefficients are characteristic of the EMAP and ASIMD models.

Evaluation of transboundary transport

In addition to the comparison of calculation results with measurements the intercomparison procedure included the evaluation of Cd transboundary transport for selected countries, in particular, Italy, Poland and United Kingdom.

On the basis of the total deposition values a fraction of the national emission transported outside the country (export) was evaluated. Besides that a fraction of the total deposition on the selected country (import) from all European sources located outside the borders of the country was calculated. These results are summarized in Table 8.

Table 8. The fraction of country emission exported outside the borders of the country and the fraction of total deposition attributed to the sources located outside the country

Cd Export (% of emission)	ASIMD	EMAP	GKSS	TREND
Poland	56%	44%	56%	64%
Italy	71%	64%	73%	74%
United Kingdom	69%	56%	65%	68%
Cd Import (% of total deposition)				
Poland	28%	23%	40%	39%
Italy	10%	9%	25%	23%
United Kingdom	9%	6%	10%	7%

It can be noted that ASIMD, GKSS and TREND models provide rather close estimates of the emission export values. Estimations of EMAP model are somewhat lower comparing to other models. However, the differences between the models for the export values are relatively small being on the whole within a factor of two. Partly this can be explained by the fact that the removal processes at these rather short distances are relatively less important in comparison to other processes like dispersion and transport. Hence possible differences between the models in this field are not noticed.

The import values obtained by EMAP and ASIMD, on one hand, and GKSS and TREND, on the other hand, are rather close. At the same time the difference in estimates between these two groups is more significant. The models in the first group are Eulerian models and in the

second are Lagrangian ones. It is not clear if this could explain the above import differences. Contrary to the export values, the import values are largely dependent on the parameterizations of the removal processes like the assumptions on particle distribution, deposition velocities per particle size etc.

Conclusions and recommendations

On the basis of the results obtained the following conclusions and recommendations were made. Four regional atmospheric transport models for cadmium took part in the intercomparison study. Calculations were made for 1990 using high estimates of cadmium emissions of ESQUAD project. The comparison with measurement was made with the data of observations taken from CCC database.

1. The models manifested rather close results testifying to similar approaches in modelling of cadmium transboundary transport. The comparison results do not reveal any preference of one model over others. Some models provide better results of air concentrations some - of concentrations in precipitation and wet depositions.

2. ASIMD model, developed in MSC-E and used for simulation of HM transport within the EMEP region, demonstrates rather good agreement with other participated models.

3. The comparison with observations indicates modelling results of all the models range within a factor of 2 with regard to measurements. However, it should be noted that available HM measurements are rather scarce.

4. The assessment of cadmium transboundary transport within the EMEP region shows similar results for the export values (within 20-30%) calculated by the models but some differences for the import values (factor of 2). These differences result from the differences in parameterizations of and assumptions on the emission, transport, dispersion and removal processes used in the models.

As recommendations for the next stages of the model intercomparison it can be suggested:

- to extend the measurement database and to use recent estimates of HM emissions in Europe;

- as far as emission and measurement data are being accumulated to consider a possibility to repeat lead and cadmium model intercomparison at the next stages.

- to indicate the importance of the parameters in the emission, transport, dispersion and removal processes, sensitivity tests with the ASIMD model should be carried out. In this way, for instance, the uncertainty in the import and export values can be quantified.

References

Axenfeld F. et al. [1992] Test-emissionsdatenbasic der Spurenelemente As, Cd, Hg, Pb, Zn und der speziellen organischen verbindungen Lindan, HCB, PCB, und PAK fur Modellrechnungen in Europe // Report N UBA-FB 104 02 588, Dornier GmbH.

Berdowski J.J.M., J. Baas, J.P.J. Bloos, A.J.H. Visschedijk and P.Y.J. Zandveld [1997] The European emission inventory of heavy metals and persistent organic pollutants for 1990. TNO Institute of Environmental Sciences, Energy Research and Process Innovation, Apeldoorn, UBA-FB report 104 02 672/03, p.239.

Berg T., Hjellbrekke A-G. and N. Ritter [1997] Heavy metals and POPs within the ECE region. Additional data. EMEP/CCC-Report 9/97, ref. O-95038, August.

Graziani G., Galmarini S.,Grippa G., and W. Klug [1998] Real-time long-range dispersion model evaluation of the ETEX second release, WMO, JRC, International Atomic Energy Agency.

Hanna S.R. [1988] Air quality model evaluation and uncertainty, JAPCA, 38, 406-412.

Nriagu J.O. [1989] A global assessment of natural sources of atmospheric trace metals. *Nature*, 338, 47-49.

Nriagu J.O. and J.M. Pacyna [1988] Quantitative assessment of worldwide contamination of air, water and soils by trace metals. *Nature*, 333, 134-139.

Pacyna J.M. [1995] Emission inventoring for heavy metals in the ECE. In: Heavy Metals Emissions. State-of-the-Art Report, Economic Commission for Europe, Convention on Long-range Transboundary Air Pollution, Prague, June 1995, pp. 33-50.

Ryaboshapko A. G. and P.A. Bryukhanov [1993] Heavy metals and high-molecular organic compounds in the atmosphere. MSC-E/EMEP report 5/93, Moscow, 38 ps.

Skotnikova O.G. and S.A. Smirnova [1995] Cd in the environment. Emission, transport, impacts. EMEP/MSC-E, Moscow.

van den Hout [1994] Main report of ESQUAD project, RIVM rep.722401003, IMW-TNO rep.R93/329.

Annex A

Figures and tables

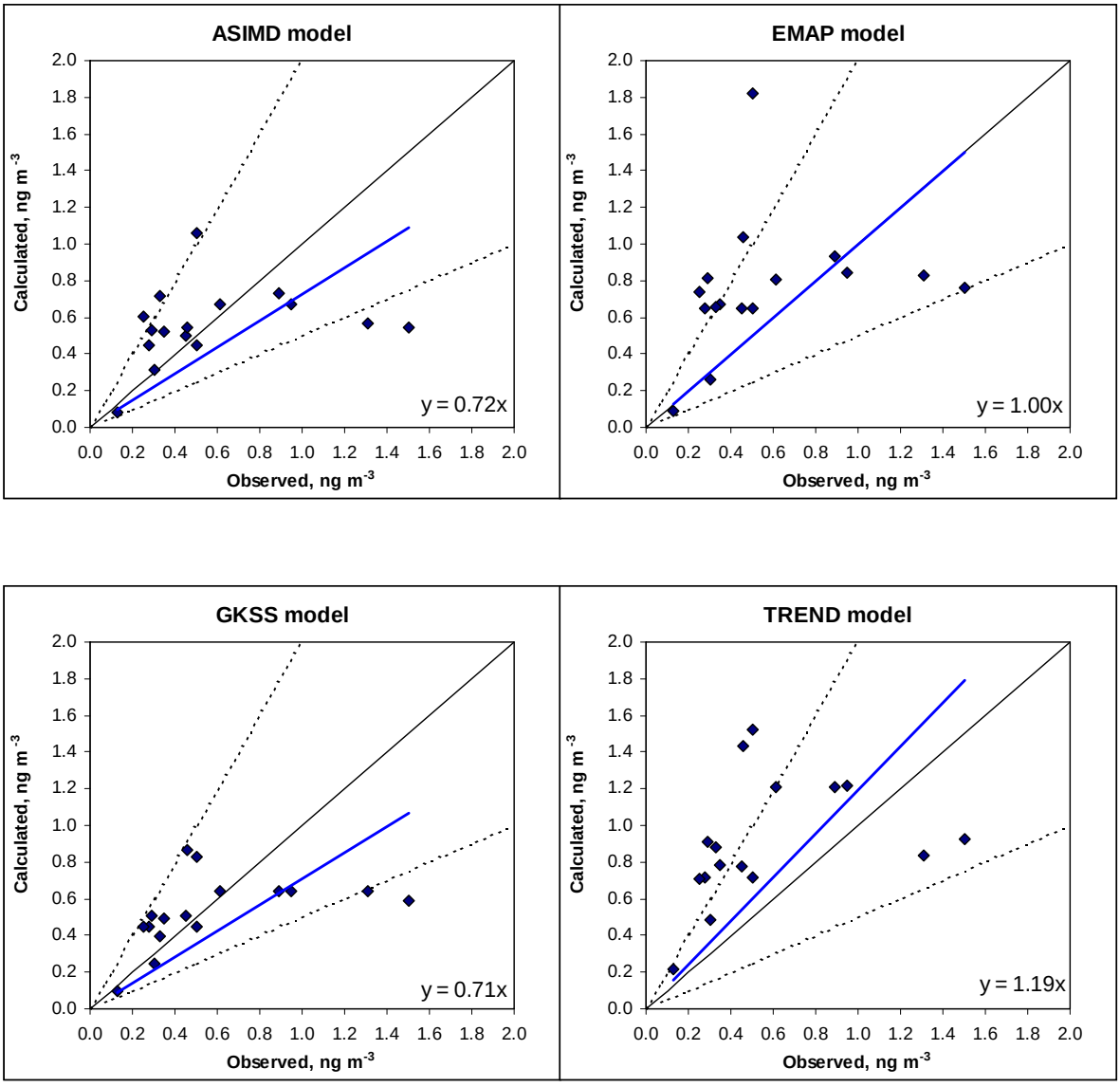

Figure A1. Scatter plots of calculated and measured Cd air concentrations. Dashed lines define the 'factor of 2' band, solid line is 1:1 line

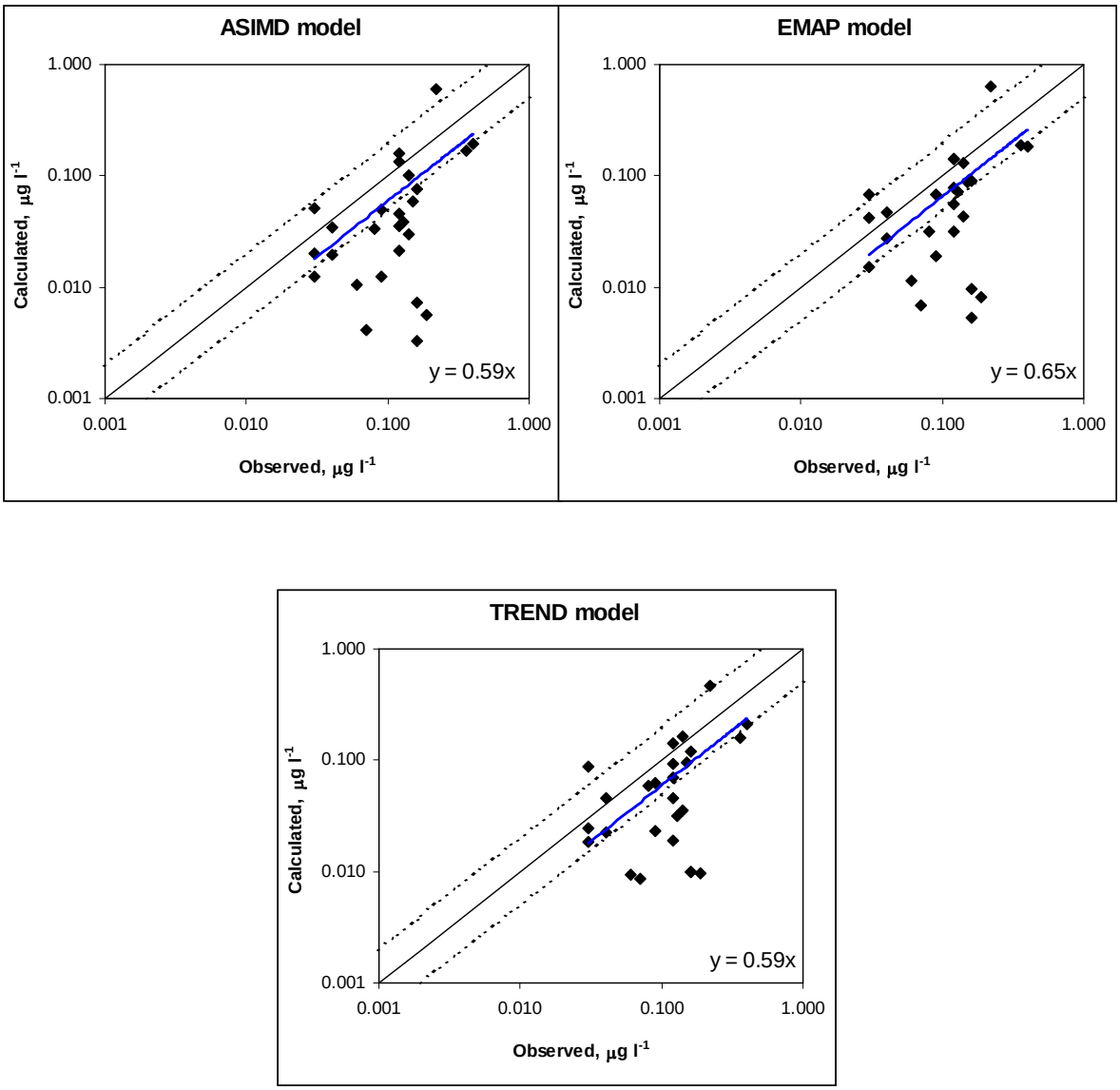

Figure A2. Scatter plots of calculated and measured Cd concentrations in precipitation. Dashed lines define the 'factor of 2' band, solid line is 1:1 line

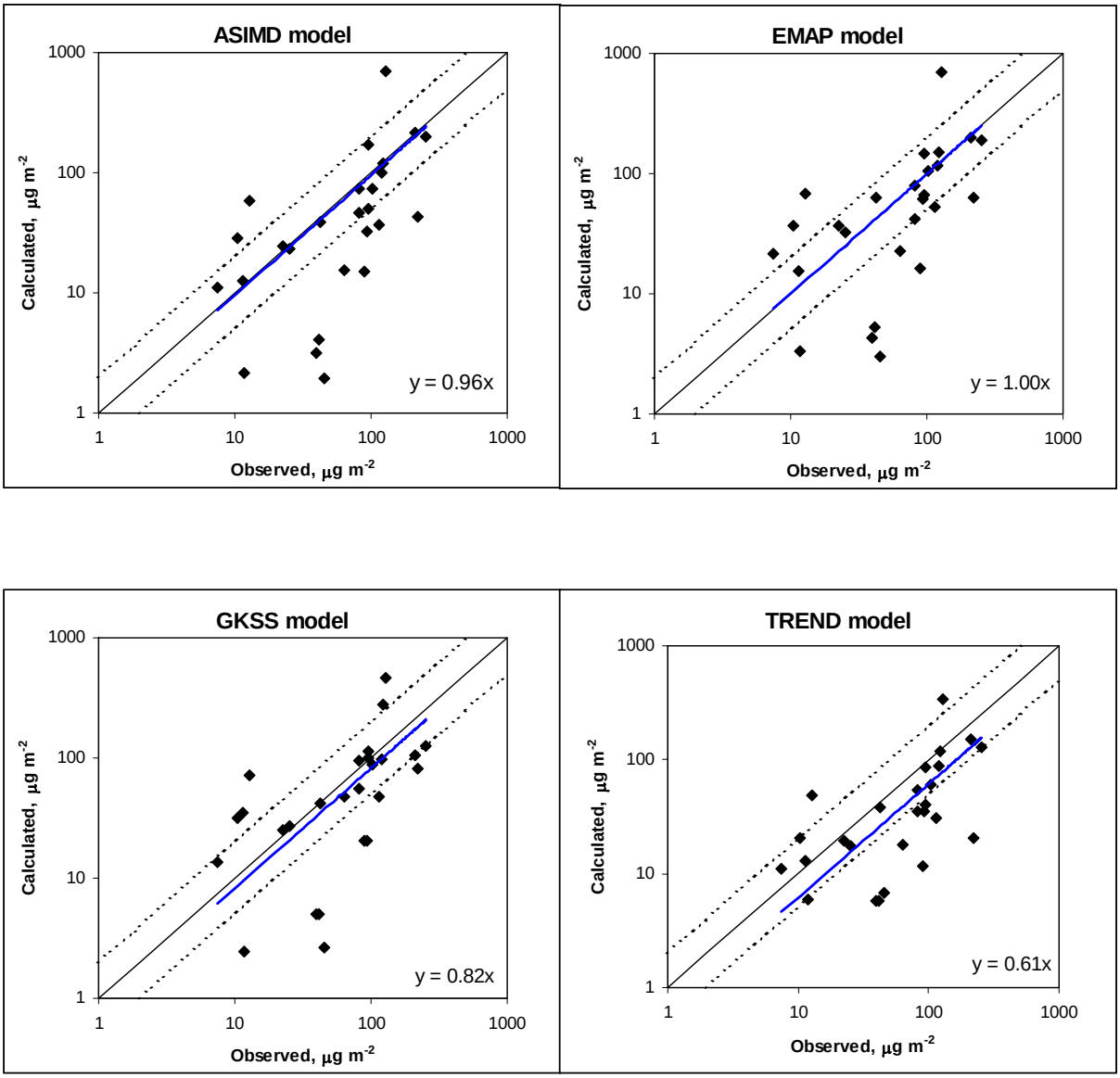

Figure A3. Scatter plots of calculated and measured Cd wet deposition. Dashed lines define the 'factor of 2' band, solid line is 1:1 line

Table A1. The list of sites with available Cd measurements for 1990

No.	Site	Site Name	Height	Samples	Samples below	Sampling period	Measurements
1	CS1	Svratouch	737	11	0	Monthly	Air
2	CS3	Kosetice	633	12	0	Monthly	Air
3	DK31	Ulborg	10	12	0	Monthly	Prec
4	FI90	Haapasaari	15	11	0	Monthly	Prec
5	FI91	Hailuoto	4	11	1	Monthly	Prec
6	FI92	Hietajarvi	173	7	0	Monthly	Prec
7	FI93	Kotinen	158	6	0	Monthly	Prec
8	FI94	Pesosjarvi	257	7	0	Monthly	Prec
9	FI95	Vuoskojarvi	147	7	0	Monthly	Prec
10	FR90	Porspoder	0	12	0	Monthly	Prec
11	DE1	Westerland	12	7/12	0/0	Monthly	air/prec
12	DE2	Langenbrugge	74	334	0	Daily	Air
13	DE3	Schauinsland	1205	12	0	Monthly	Air
14	DE4	Deuselbach	480	12	0	Monthly	Air
15	DE5	Brotjacklriegel	1016	12	0	Monthly	Air
16	NL10	Vreedepeel	-	12	1	Monthly	Prec
17	NL2	Witteveen	18	12	5	Monthly	Prec
18	NL9	Kollumerwaard	0	12	3	Monthly	Prec
19	NO1	Birkenes	190	12	0	Monthly	Prec
20	NO30	Jergul	255	12	0	Monthly	Prec
21	NO39	Kraavatn	210	12	0	Monthly	Prec
22	NO41	Osen	440	12	0	Monthly	Prec
23	NO44	Nordmoen	200	12	0	Monthly	Prec
24	NO47	Svanvik	30	12	0	Monthly	Prec
25	NO91	Noatun	60	12	0	Monthly	Prec
26	*NO96*	*Namsvatn*	*500*	*4*	*0*	*Monthly*	*Prec*
27	*NO97*	*Solhomfjell*	*260*	*4*	*0*	*Monthly*	*Prec*
28	*PT1*	*Braganca*	*691*	*29*	*29*	*Daily*	*Prec*
29	*PT3*	*V.d. Castelo*	*16*	*49*	*49*	*Daily*	*Prec*
30	SK2	Chopok	2008	11	0	Monthly	Air
31	SK4	Stara Lesna	808	11	0	Monthly	Air
32	SK5	Liesek	892	12	0	Monthly	Air
33	SE12	Aspvreten	20	12	0	Monthly	Prec
34	SE5	Bredkalen	404	12	0	Monthly	Prec
35	SE98	Svartedalen	0	12	0	Monthly	Prec
36	SE99	Arup	0	12	0	Monthly	Prec
37	*CH1*	*Jungfraujoch*	*3573*	*8*	*0*	*Annual*	*Air*
38	CH2	Payerne	510	8	0	Annual	Air
39	CH3	Tanikon	540	8	0	Annual	Air
40	CH4	Chaumont	1130	5	0	Annual	Air
41	CH5	Rigi	1030	5	0	Annual	Air
42	GB90	East Ruston	5	12/12	1/0	Monthly	air/prec
43	GB91	Banchory	120	12/12	2/1	Monthly	air/prec
44	GB93	Staxton Wold	35	12	0	Monthly	Prec
45	*GB94*	*Lough Erne*	*35*	*12*	*0*	*Monthly*	*Prec*

Table A2. Results of the comparison for Cd air concentrations, ng/m^3

Sites	**Obs**	**ASIMD**	**EMAP**	**GKSS**	**TREND**	**Mean**	**Obs/Mod**
CH2	0.50	0.45	0.65	0.45	0.72	0.55	0.90
CH3	0.45	0.50	0.65	0.51	0.78	0.58	0.78
CH4	0.28	0.45	0.65	0.45	0.72	0.51	0.55
CH5	0.25	0.61	0.74	0.45	0.71	0.55	0.45
CS1	1.50	0.54	0.76	0.59	0.92	0.86	1.74
CS3	1.31	0.57	0.83	0.64	0.84	0.84	1.57
DE1	0.30	0.31	0.26	0.24	0.49	0.32	0.93
DE2	0.46	0.54	1.04	0.86	1.43	0.87	0.53
DE3	0.29	0.53	0.82	0.51	0.91	0.61	0.47
DE4	0.50	1.06	1.82	0.83	1.52	1.15	0.44
DE5	0.35	0.52	0.67	0.50	0.78	0.56	0.62
GB90	0.33	0.71	0.66	0.40	0.88	0.60	0.55
GB91	0.13	0.08	0.09	0.10	0.22	0.12	1.05
SK2	0.61	0.67	0.81	0.64	1.21	0.79	0.77
SK4	0.95	0.67	0.84	0.64	1.22	0.87	1.10
SK5	0.89	0.73	0.93	0.64	1.21	0.88	1.01
Mean arithm	0.57	0.56	0.76	0.53	0.91	0.67	0.84
Mean geom	0.47	0.50	0.66	0.48	0.84	0.60	
Variance	0.146	0.041	0.125	0.035	0.108	0.058	
Std dev	0.38	0.20	0.35	0.19	0.33	0.24	
Correlation		0.28	0.25	0.46	0.34	0.60	
FB		-0.02	0.29	-0.07	0.46	0.16	
FSD		-1.13	-0.16	-1.22	-0.30	-0.86	
FAC2		69%	69%	88%	56%	81%	
Slope		0.72	1.00	0.71	1.19		
NMSE		0.45	0.55	0.39	0.55	0.27	

Table A3. Results of the comparison for Cd concentrations in precipitation, μg/l

	Obs	ASIMD	EMAP	TREND	Mean	Obs/Mod
DE1	0.150	0.059	0.087	0.096	0.121	1.24
DK31	0.090	0.050	0.067	0.063	0.102	0.88
FI90	0.120	0.046	0.079	0.069	0.087	1.38
FI91	0.120	0.035	0.056	0.045	0.061	1.97
FI92	0.040	0.035	0.047	0.046	0.057	0.70
FI93	0.030	0.052	0.068	0.088	0.092	0.33
FI94	0.030	0.020	0.042	0.024	0.036	0.84
FI95	0.070	0.004	0.007	0.009	0.010	7.09
FR90	0.040	0.019	0.027	0.023	0.060	0.66
GB90	0.400	0.194	0.185	0.208	0.246	1.62
GB91	0.130	0.039	0.073	0.032	0.061	2.14
GB93	0.360	0.170	0.187	0.159	0.232	1.55
NL10	0.220	0.601	0.627	0.465	0.871	0.25
NL2	0.140	0.100	0.129	0.162	0.322	0.43
NL9	0.160	0.076	0.090	0.121	0.170	0.94
NO1	0.120	0.021	0.032	0.019	0.039	3.07
NO30	0.160	0.003	0.005	0.010	0.011	15.17
NO39	0.060	0.011	0.012	0.009	0.021	2.82
NO41	0.090	0.012	0.019	0.023	0.031	2.88
NO44	0.140	0.030	0.043	0.035	0.045	3.13
NO47	0.160	0.007	0.010	0.010	0.013	12.09
NO91	0.190	0.006	0.008	0.010	0.012	15.42
SE12	0.120	0.133	0.140	0.092	0.138	0.87
SE5	0.030	0.012	0.015	0.018	0.027	1.13
SE98	0.080	0.033	0.031	0.059	0.077	1.04
SE99	0.120	0.157	0.140	0.143	0.186	0.65
Mean arithm	0.130	0.074	0.086	0.078	0.120	1.08
Mean geom	0.10	0.03	0.05	0.04	0.06	
Variance	0.008	0.014	0.014	0.009	0.029	
Std dev	0.09	0.12	0.12	0.09	0.17	
Correlation		0.48	0.46	0.52	0.44	
FB		-0.55	-0.41	-0.49	-0.07	
FSD		0.57	0.60	0.15	1.15	
FAC2		27%	50%	50%	54%	
Slope		0.59	0.65	0.59		
NMSE		1.54	1.30	1.04	1.52	

Table A4. Results of the comparison for Cd wet deposition, $\mu g/m^2$

	Obs	ASIMD	EMAP	GKSS	TREND	Mean	Obs/Mod
DE1	103.0	72.7	105.0	89.1	61.0	82.0	1.26
DK31	95.4	50.3	66.1	99.8	39.8	64.0	1.49
FI90	42.6	38.4	63.4	42.0	38.4	45.6	0.94
FI91	22.4	24.7	36.7	25.2	19.5	26.5	0.84
FI92	10.4	28.3	36.6	31.8	20.7	29.4	0.35
FI93	12.8	58.4	67.4	71.2	48.4	61.4	0.21
FI94	7.5	11.2	21.4	13.7	10.9	14.3	0.52
FI95	11.8	2.2	3.3	2.4	5.9	3.5	3.40
FR90	25.3	23.5	32.4	26.8	17.3	25.0	1.01
GB90	210.0	216.0	199.0	105.0	151.0	167.8	1.25
GB91	93.2	32.8	61.1	20.7	34.8	37.4	2.50
GB93	254.0	199.0	189.0	125.0	128.0	160.3	1.59
NL10	129.0	702.0	694.0	466.0	340.0	550.5	0.23
NL2	122.0	121.0	149.0	281.0	119.0	167.5	0.73
NL9	120.0	101.0	116.0	98.3	89.3	101.2	1.19
NO1	221.0	43.2	62.9	82.1	20.6	52.2	4.23
NO30	45.2	2.0	3.0	2.7	6.9	3.6	12.48
NO39	89.8	15.0	16.2	20.7	11.5	15.9	5.67
NO41	63.9	15.4	22.9	47.7	17.9	26.0	2.46
NO44	115.0	36.9	52.6	47.7	30.5	41.9	2.74
NO47	41.1	4.1	5.2	5.0	5.8	5.0	8.21
NO91	39.3	3.2	4.3	5.0	5.8	4.6	8.63
SE12	82.4	74.4	78.7	55.0	54.3	65.6	1.26
SE5	11.4	12.7	15.3	34.7	13.1	19.0	0.60
SE98	82.2	46.8	42.2	95.0	35.0	54.8	1.50
SE99	95.7	172.0	147.0	114.0	85.5	129.6	0.74
Mean aritm	82.6	81.0	88.1	77.2	54.26	75.2	1.10
Mean geom	55.3	32.9	42.0	39.6	30.2	37.5	
Variance	4288	18854	17695	9353	4828	11488	
Std dev	65	137	133	97	69	107	
Correlation		0.44	0.43	0.44	0.51	0.46	
FB		-0.02	0.07	-0.07	-0.41	-0.09	
FSD		1.26	1.22	0.74	0.12	0.91	
FAC2		54%	54%	46%	54%	54%	
Slope		0.59	0.65	1.77	0.94		
NMSE		2.29	1.98	1.28	1.18	1.52	

Table A5. Results of the comparison for precipitation amount, mm

Sites	**Obs**	**ASIMD**	**EMAP**	**TREND**	**Mean**	**Obs/Mod**
DE1	687	1226	1204	634	858	0.80
DK31	1060	1004	982	637	765	1.39
FI90	355	842	804	553	618	0.57
FI91	187	700	658	432	506	0.37
FI92*	260	820	777	452	592	0.44
FI93*	427	1127	996	548	780	0.55
FI94*	250	557	511	449	440	0.57
FI95*	169	524	483	693	456	0.37
FR90	633	1218	1182	765	830	0.76
GB90	525	1113	1076	726	795	0.66
GB91	717	841	842	1088	745	0.96
GB93	706	1171	1011	805	822	0.86
NL10	586	1168	1107	731	817	0.72
NL2	871	1210	1155	735	853	1.02
NL9	750	1334	1293	738	904	0.83
NO1	1862	2038	1991	1090	1522	1.22
NO30	276	598	562	694	492	0.56
NO39	1519	1429	1409	1238	1115	1.36
NO41	711	1252	1218	772	979	0.73
NO44	825	1247	1218	866	1001	0.82
NO47	264	560	536	583	467	0.56
NO91	207	560	535	604	473	0.44
SE12	687	559	562	588	500	1.37
SE5	380	1024	1007	716	830	0.46
SE98	1028	1414	1353	589	968	1.06
SE99	798	1096	1050	598	780	1.02
Mean	644	1024	981	705	766	0.84
Correlation		0.83	0.85	0.71	0.88	

* - incomplete data sets for 1990 (See table A1).

Annex B

Description of models

Description of EMAP model

Basic information

Model name: **EMAP** (Eulerian Model for Air Pollution)

Model versions and status: Three versions: EMAP_S (SO2-SO4), EMAP_A (aerosol, Pb, POP), EMAP_E (passive inert gas)

Contact person: Dimiter Syrakov

Institution: National Institute of Meteorology and Hydrology, Bulgarian Academy of Sciences

Contact address: 66 Tzarigradsko chaussee, 1784 Sofia, Bulgaria

Phone number: +359 2 975 39 86/87/88/91/92

Fax number: +359 2 88 03 80 / 88 44 94

E-mail address: dimiter.syrakov@meteo.bg

Intended field of application: Simulation of pollutant dispersion at the local-to-regional and regional-to continental scale

Model type and dimension: Three-dimensional, Eulerian

Model description summary: EMAP is a simulation model, which allows describing the dispersion of multiple pollutants. The processes as horizontal and vertical advection, horizontal and vertical diffusion, dry deposition, wet removal, gravitational settlings (aerosol version) and simplest chemical transformation (sulphur version) are accounted for in the model. Within EMAP, the semi-empirical diffusion-advection equations for scalar quantities are solved. The governing equations are solved in terrain-following co-ordinates. Non-equidistant grid spacing is settled in vertical directions. The numerical solution is based on discretization applied on a staggered grids. Conservative properties are fully preserved within the discrete model equations. Advective terms are treated with the TRAP scheme, which is a Bott type one. Displaying the same simulation properties as the Bott scheme (explicate, conservative, positively definite, transportable, limited numerical dispersion), the TRAP scheme occur to be several times faster. The advective boundary conditions are zero at income and "open boundary" at outcome flows. Turbulent diffusion is described with the simplest schemes. The bottom boundary condition for the vertical diffusion equation is the dry deposition flux, the top boundary condition is optionally "open boundary" and "hard lid" type. The lateral boundary conditions for diffusion are "open boundary" type. In the surface layer a parameterization is applied permitting to have the first computational level at the top of SL. It provides a good estimate for the roughness level concentration and accounts also for the act of continuous sources on the earth surface.

Temporal resolution: time step - 15 seconds to 30 minutes, simulated time period - some hours to month and year

Horizontal resolution: grid size 500 to 150000 m, domain dimension - 20 to 5000 km

Vertical resolution: log-linear gridding, parameters defined by the user.

Schemes

Advection: TRAP scheme, flux-type, 1st order explicit in time, conservative, transportive, positively defined, limited numerical dispersion; 3rd order Bessel polynomial used for fitting concentration. In the vertical advection correction for divergency is introduced.

Diffusion: Simplest implicit (vertical) and explicit (horizontal) schemes with accuracy of 1st order in time and 2nd order in space. Horizontal diffusion coefficients are constants (defined by the user), the vertical diffusion coefficient is a field. The dry deposition velocity is prescribed at each grid point for each pollutant.

Wet removal: Simplest decay approach, coefficient depending on rain intensity

Aerosol specific processes: The gravitational settling and the wet removal of pollutants carried by aerosols are described on the base of Galperin's parameterization.

Solution technique: The discretized equations are solved numerically on an Arakawa C-type staggered grid. If (*i,j,k*) is the mass point, *U* is defined in point (*i*+1/2,*j,k*), *V* - in (*i,j*+1/2,*k*), *W* and K_Z - in (*i,j,k*+1/2). One dimensional schemes are created for every dimension for advection and diffusion. They are applied sequentially for each time step (splitting approach), the order reversed at the next time step. Source concentration is added at every two time steps.

Input requirements

Emissions: The emissions are provided in mass units per second. For the high sources (*i,j,h*, strength) is necessary, for the area sources: (*i,j*, strength).

Meteorology: Only 850 hPa U-,V- and Teta-fields as well as surface Teta-field are necessary as meteorological input. A simple PBL model is built in EMAP producing U-, V-, W- and K_Z-profiles at each grid point. It provides also u* and SL universal profiles necessary in *SL* parameterization. The roughness and Corriolis parameter fields are preset additional input to the PBL model.

Topography: Orography height, surface type (sea-lend mask) are to be provided for each grid location

Initial conditions: Initial concentration field is optionally introduced (spin-up field)

Other input requirements: A run-file with control data is read

Output quantities: Concentration and deposition fields in SURFER's GRD-format layer by layer. Intermediate and final outputs are provided. Averaging of concentrations for predefined period is available.

User interface availability: PC-DOS operating system

Previous applications: Applied for studying annual acid loads in the region of south-eastern Europe. Applied for calculating Bulgarian impact of lead and benzo(a)pyrene in the same region for different years.

Documentation status: Described in different reports and conference presentations (see Reference). No documentation available for the moment.

Validation and evaluation: Participation in ETEX-II intercalibration study - ranged 9th among 34 models. Validated on the data base of 1996 EMEP/MSC-E intercalibration of heavy metal models.

Portability: IBM PC compatible computers - 486 or Pentium

CPU time: One year simulation over the EMEP 50×50 km grid (111×117 points), one pollutant, 5 layer version, lasts 12 hours on 120 MHz Pentium

Storage: For the same case: 16 Mbytes RAM. Disk space: 2-5 Mbyts needed for the output files.

References

Bulgarian contribution to EMEP, Annual reports for 1994, 1995, 1996, 1997, NIMH, EMEP/MSC-E, Sofia-Moscow.

Syrakov D. [1995] On a PC-oriented Eulerian Multi-Level Model for Long-Term Calculations of the Regional Sulphur Deposition, in Gryning S.E. and Schiermeier F.A. <Ed.> Air Pollution Modelling and its Application XI, NATO · Challenges of Modern Society, Vol. 21, Plenum Press, N.Y. and London, pp. 645-646.

Syrakov D. [1996] On the TRAP advection scheme - Description, tests and applications, in Geernaert G., A.Walloe-Hansen and Z.Zlatev <Eds.>, Regional Modelling of Air Pollution in Europe. Proceedings of the first REMAPE Workshop, Copenhagen, Denmark, September 1996, National Environmental Research Institute, Denmark, pp. 141-152.

Syrakov D. and M. Galperin [1997] On a new Bott-type advection scheme and its further improvement, in H. Hass and I.J. Ackermann <Eds.>, Proc. of the first GLOREAM Workshop, Aachen, Germany, September 1997, Ford Forschungszentrum Aachen, pp. 103-109.

Syrakov D. and M. Galperin [1997] A model for airborne poli-dispersive particle transport and deposition, Proc. of 22nd NATO/CCMS International Technical Meeting on Air Pollution Modelling and its Application, 2-6 June 1997, Clermont-Ferrand, France, 111-118.

Syrakov D. and M. Prodanova [1997] Bulgarian Long-range Transport Models - Simulation of ETEX First Release, in K.Nodop <Ed.>, Proc. of ETEX Symposium on Long-range Atmospheric Transport, Model. Verification and Emergency Response, 13-16 May 1967, Vienna (Austria), Office for Official Publications of the European Communities, Luxembourg, ISBN 92-828-0669-3, 141-144.

Syrakov D. and D. Yordanov [1997] Parameterization of SL Diffusion Processes Accounting for Surface Source Action, Proc. of 22nd NATO/CCMS International Technical Meeting on Air Pollution Modelling and its Application, 2-6 June 1997, Clermont-Ferrand, France, 111-118.

Yordanov D., Syrakov D. and G. Djolov [1983] A barotropic planetary boundary layer, Boundary Layer Meteorology, 25, 363-373.

Description of GKSS model

For long range transport of atmospheric pollutants and long term averages of air pollutant concentrations and depositions Lagrangian type models, where the horizontal dispersion is described by a large number of trajectories, have been proven to be an appropriate tool. In this category the EMEP/MSC-W model was one of the first operational models. It was developed at the Norwegian Meteorological Institute in the framework of the `Co-operative programme for monitoring and evaluation of the long range transmission of air pollutants in Europe` [*Eliassen and Saltbones,* 1983]. After comprehensive tests and validations the model has been used on a routine basis for the assessment of the quantity of sulphur pollution crossing national boundaries between European countries. The results show that average concentrations and fluxes of sulphur dioxide and particulate sulphate are predicted reasonably well.

On this background and due to the fact that the transport and deposition processes for trace metals and particulate sulphate are similar it was decided to apply the EMEP-model for the calculation of the atmospheric input of trace metals into the North Sea and the Baltic Sea.

The basic transport equation for the concentration q of a trace metal in the atmosphere is:

$$\frac{Dq}{dt} = -\left(\frac{v_d}{h} + K_W\right)q + (1-\alpha)\frac{Q}{h}$$

The operator D/dt is the total (Lagrangian) time derivative. Q denotes the source strength, i.e. the emission per unit area and time. The remaining symbols are as follows:

α - source strength reduction factor;

v_d - dry deposition velocity, $m \cdot s^{-1}$;

K_W - wet deposition rate, s^{-1};

h - mixing height, m.

In Lagrangian models such as GKSS instantaneous homogenous mixing of emitted material throughout the mixing layer is assumed. However, in reality this mixing process requires some time, thus affecting the `local deposition` in the emission grid square. This especially applies to species with large deposition velocities emitted at low heights. The resulting faster depletion due to enhanced deposition is taken into account by a source strength reduction factor α. For lead with a high contribution of low height emissions due to gasoline combustion in vehicles α is assumed to be 0.15.

In principle the dry deposition v_d of trace metals is not a unique constant for each species. Its value is a function of the particle size, the structure of the underlying surface and the meteorological conditions. In case of sea surfaces there may also be a significant spray particle formed by breaking waves provide an example for such transport. Nevertheless a constant dry deposition velocity for each trace metal is applied in the model (0.4 cm/s for cadmium).

In Lagrangian models the wet deposition process is usually modelled by means of a single scavenging coefficient K_W, which is related to the scavenging ratio W (concentration in precipitation/concentration in air) by:

$K_W = W\,P/h$

where P - precipitation rate, m/s;

h - mixing height, m.

W includes in-cloud scavenging as well as below-cloud scavenging. In the model a scavenging ratio W = 700000 is applied for cadmium.

The mixing height h is defined as the height up to the lowest stable layer above 200 m. A layer is defined as stable in this context if the vertical temperature gradient, $dT/dz > -5.0 \times 10^{-3}$ [K·m^{-1}]. The model estimates a variable mixing height from 12 GMT radiosonde data and from a parameterization of the exchange of pollution, which takes place between the boundary layer and the free troposphere. Details are described in [*Gronas and Hellevik*, 1982].

The model is a receptor-oriented model. The 96h-backward trajectories are derived from the windfield in the 150x150 km^2 grid system (GKSS/MSC-W). They arrive at 720 receptor points every 6 h. Most of the receptor points are the center points of grid elements in which the emissions and the meteorological data are given. The others are the exact locations of measurement stations.

During time periods when synoptic observations are used to generate the meteorological input, the trajectories are calculated from the 850 hPa wind field. From measurements it is known that the concentration of pollutants in the atmosphere decreases rapidly with height. In general the concentration weighted transport height will be lower than the 850 hPa level. Therefore since 1985, when the input data are obtained from the limited area prediction model the trajectories are calculated from the 925 hPa (~800 m altitude) windfield, which is considered to be representative for the transport wind in trajectory models.

The precipitation fields are important elements in long range transport models, because often more than 50% of the atmospheric pollutants are deposited by precipitation. However, precipitation from single convective clouds as well as from large frontal systems is very intermittent and spatially varying, when it is compared with the density in space and time of the synoptic rain collector network. So, synoptic observations are insufficient for a 6h-analysis in the EMEP grid system of 150x150 km^2, especially for the North Sea and the Baltic Sea where no observations are considered to be more reliable since 1985, when the precipitation fields were derived from the weather prediction model.

The mixing height fields are generated by an objective analysis of about 100 radiosonde reports. 10 of these are from isolated islands or ships in the Atlantic Ocean. Again, it appears that those data are spatially too sparse to give a reasonably detailed analysis of the mixing height field, and that a significant improvement of those data can be expected, when the whether prediction model is used.

References

Eliassen A. and J.Saltbones [1983] Modelling of long-range transport of sulphur over Europe: a two year model run and some model experiments. *Atmospheric Environment*, Vol.17, N8, pp.1457-1483.

Gronas S. and O.E.Hellevik [1982] A limited area prediction model at the Norwegian Meteorological Institute. *Det Norske Meteorologiske Institutt*, Technical Report, N61.

Description of ASIMD model

The present version of ASIMD model is of Eulerian type, it was developed within the framework of the Co-operative Programme for Monitoring and Evaluation of the Long-range Transmission of Air Pollutants in Europe for calculations of HM transboundary transport in the atmosphere and their deposition.

The model is emission driven and includes advection transport, turbulent diffusion, wet and dry deposition. The transport equation is written in form:

$$\frac{\partial C}{\partial t} = u \cdot \frac{\partial C}{\partial x} + v \cdot \frac{\partial C}{\partial t} = K_H \cdot \left(\frac{\partial^2 C}{\partial x^2} + \frac{\partial^2 C}{\partial y^2} \right) + \frac{\partial}{\partial z} K_Z \cdot \frac{\partial C}{\partial z} - \Lambda \cdot C + Q \,,$$

where C - concentration of a pollutant;

u,v - wind speed components;

K_H, K_Z - turbulent diffusion coefficients in horizontal and vertical direction, respectively;

Λ - washout coefficient;

Q - emission.

The transport equation is solved by splitting to physical processes [*Pekar*, 1996].

In the previous model version the vertical structure was divided into four unequal layers of 100, 300, 700 and 1000 m covering the whole boundary layer. In the present version one more layer of 1800 m thick was added. The middle of this layer corresponds to 700 hPa.

Anthropogenic emissions of cadmium can be released from surface and elevated sources. It is assumed that 50% pollutant is emitted to the first and second model layers. Seasonal variations of cadmium emissions as well as natural emission are not considered.

Pollution advection defining the transport in horizontal direction is described as suggested in [*Pekar*, 1996]. The transport can be to two downwind neighboring cells and to a downwind cell along the diagonal.

Pollution diffusion in horizontal direction is treated by the approach described by [*Izrael et al*., 1980]. Vertical diffusion is described by an implicit scheme. Diffusion equation is solved by the sweep method. In the atmosphere there are zones of convergence and divergence of air fluxes with systems of low and high pressure associated with a large-scale vertical air motions. The velocities of these vertical motions are calculated at each time step on the basis of air mass balance conservation in each cell on the assumption of air mass non-compression. The upper boundary of the model air reservoir is open for the exchange with the above atmosphere.

Meteorological data are prepared by Hydrometeorological Centre of the Russian Federation. They include temperature and wind at 1000, 925, 850 and 700 hPa and the integral amount of precipitation near the ground surface. In model calculations for the fifth layer meteorological data on the isobaric surface of 700 hPa are used, for the fourth layer - on 850 hPa, for the third - on 950 hPa and for the

second - 1000 hPa. Wind speed and temperature in the first model layer and K_Z values are calculated in the course of the boundary layer parameterization, the detail description is given in [*Pekar*, 1996].

Dry deposition is described following the approach suggested in [*Pekar,* 1996]. The flux to the underlying surface is written in the form $F_{dry} = V_d C(1)$ where V_d is the dry deposition velocity and $C(1)$ - cadmium concentration in the first model layer. Dry deposition velocity is calculated depending on the underlying surface type, roughness parameter and wind speed.

$$V_d^{land} = (0.04 \cdot u_*^2 + 0.02) \cdot (z_0 / 10^{-3})^{0.30}$$

$$V_d^{sea} = 0.15 \cdot u_*^2 + 0.023$$

Formulas derived for cadmium and used in calculations are given below.

In these formulas z_0(m) - roughness parameter, u_* - friction velocity, V_D are calculated in cm/s.

Wet scavenging of particles carrying heavy metals is described in a classical way as a first order process:

$$\frac{\partial C}{\partial t} = -\Lambda C \, .$$

Washout coefficient is calculated in the following way:

$$\Lambda = \frac{W \cdot I}{\Delta z_i}$$

Here I - precipitation intensity;

Δz_{ip} - layer depth where washout takes place and W is washout coefficient.

It was assumed to be equal to 700 000.

The model operates with spatial resolution 50 km and time step 20 min. In calculations of the transport and deposition variations of cell areas along the latitude connected with distortions caused by the stereographic projection are taken into account.

References

Pekar M.I. [1996] Regional models LPMOD and ASIMD. Algorithms, parametrization and results of application to Pb and Cd in Europe scale for 1990. EMEP/MSC-E Report 9/96.

Izrael Yu.A., Mikhailova J.E. and A.Ja. Pressman [1980] The model for operational calculations of transboundary fluxes of anthropogenic pollution (sulphur dioxide and sulphates). Reports of the USSR Academy of Sciences v.253, N.4, pp.848-852

Description of the TREND model

The TREND model [*Van Jaarsveld*, 1995] used in this intercomparison has been used in previous studies of deposition of heavy metals to the North Sea [*Van Jaarsveld et al*, 1986; *Warmenhoven et al,* 1989; *Baart et al*, 1995], the Convention waters of OSPARCOM [*Van Pul et al.*, 1998], the Rhine catchment area [*Baart and Diederen*, 1991] and the European continent [ESQUAD project, *Van den Hout,* 1994].

The version used here (called EUTREND version 1.14) covers the entire European continent with its marginal seas and calculates deposition as function of surface characteristics. The Lagrangian-type model is driven by meteorological data obtained through the Netherlands Meteorological Institute from the European Center for Medium Range Weather Forecasting.

For calculation of an average concentration/deposition at a particular receptor point, the occurring meteorological situations are divided into 4 transport distance classes and 12 wind direction classes each divided into 6 stability/mixing height classes. For 50 regions within Europe, characteristic transport and deposition parameters are determined for each class from meteorological observations [*Potma*, 1993] using a meteorological pre-processor [*van Jaarsveld*, 1995]. In the present application, the model uses a 50×50 km grid; for each individual receptor point the transport and dispersion parameters are obtained by interpolating the data for the nearest regions.

Atmospheric processes included in the model are: emissions, dispersion, advection, chemical conversion (not relevant for the Cd calculations presented here) and wet and dry deposition. An important aspect with regard to dispersion and advection is that the model describes long range transport using well mixed trajectories while local transport and dispersion is described using a Gaussian plume model. The latter model describes the air concentration as a function of source height and meteorology related dispersion parameters but, in case of high stacks, it allows for temporarily transport of pollutants above the so-called mixed layer. Although the model can handle both (low-level) area sources and point sources, in this report all Cd emissions are assumed to take place as area sources at a height of 100m. The heat output is assumed to be 20 MW; the diurnal variations in source strength is assumed to be proportional to the diurnal variations in industrial activity (i.e. ratio between daily maximum/minimum emission 1.9).

With respect to deposition, the model describes the removal rates of particle bound pollutants as a function of the particle size. During transport the evolution of the distribution to smaller particles is taken into account. In TREND particles are distributed over 5 size classes each having a specific particle diameter and specific deposition properties. The dry deposition parameters are taken from the model of *R.Williams* [1982] for water surfaces and the model of *G.Sehmel and W.Hodgson* [1979] for land surfaces.

For the wet deposition process distinction is made between in-cloud and below cloud removal. The latter process is parameterized using a description given by *A.Janssen and H.Ten Brink* [1985] using a drop-particle collision efficiencies given by *W.Slinn* [1977]. For transport distances of more than about ten kilometer the combined effect of in- and below-cloud scavenging is parameterized using a

scavenging rate during precipitation: $\Lambda = WR/H$, where W is an (empirical) scavenging ratio, R is the rain intensity and H the mixing height. An effective scavenging rate, Λ_{eff}, is estimated taking into account the intermittent nature of rain where it is assumed that the distribution of wet and dry periods over the source-receptor traject follows a Poisson distribution.

For Cd the initial particle size distribution (at the moment of emission), the mean dry deposition velocity, V_d, and mean scavenging rate, Λ_{eff}, are:

	<0.95 μm	0.95-4 μm	4-10 μm	10-20 μm	>20 μm
Cd (%)	42	33	14.5	5.9	4.6
V_d (ms^{-1})	0.00065	0.0025	0.0071	0.0132	0.067
Λ_{eff} (s^{-1})	$2.0\ 10^{-6}$	$1.5\ 10^{-5}$	$1.5\ 10^{-5}$	$1.5\ 10^{-5}$	$1.5\ 10^{-5}$

The uncertainty in the calculated concentrations and depositions, a) introduced by the modelling concepts of transport, diffusion and deposition are estimated to be about 30% including the meteorological variability; b) introduced by the choice of the particle size distribution of the emitted material at about 30-50% [*Baart et al*., 1995; *Van Jaarsveld et al.,* 1997].

References

Baart A.C. and H.S.M.A. Diederen [1991] Calculation of the atmospheric deposition of 29 contaminants to the Rhine catchment area. Report R91/219, TNO, Delft, the Netherlands.

Baart A.C., Berdowski J.J.M. and J.A. Van Jaarsveld [1995] Calculation of atmospheric deposition of contaminants on the North Sea. Report R95/138, TNO, Delft, the Netherlands.

Janssen A.J. and H.M. ten Brink [1985] Plume wash-out: modelling, calculation and validation. Report no 170, ECN, Petten, the Netherlands (in dutch).

Potma C.J.M. [1993] Description of the ECMWF/WMO Global Observational Data Set and associated data extraction and interpolation procedures. Report 722401001, RIVM, Bilthoven, the Netherlands.

Sehmel G.A. and W.J. Hodgson [1979] A model for prediction dry deposition of particles and gases to environmental surfaces. *A.I.Ch.E.Symposium Series,* 76**,** 196

Slinn W.G.N. [1977] Some approximations for the wet and dry removal of particles and gases from the atmosphere. *Water, Air Soil Pollut*, 7, 125-135.

Van den Hout K.D. (ed.) [1994] The impact of atmospheric deposition of non-acidifying compounds on the quality of European forest soils and the North Sea. Main report of the ESQUAD project. Report R93/329, TNO, Delft, the Netherlands.

Van Jaarsveld J.A. [1995] Modelling the long-term atmospheric behaviour of pollutants on various spatial scales. PH.D. thesis, University of Utrecht, the Netherlands.

Van Jaarsveld J.A., van Aalst R.M. and D. Onderdelinden [1986] Deposition of metals from the atmosphere into the North Sea: model calculations. Report 842015002, RIVM, Bilthoven, the Netherlands.

Van Jaarsveld, J.A., W.A.J. van Pul and F.A.A.M. de Leeuw. [1997] Modelling transport and deposition of persistent organic pollutants in the European region. *Atm. Env.* 31, 1011-1024.

Van Pul, W.A.J., W.A.S. Nijenhuis and F.A.A.M. de Leeuw [1998] Deposition of heavy metals to the Convention waters of OSPARCOM. Rivm report 722401016.

Warmenhoven J.P., Duiser J.A., de Leu L.Th. and C. Veldt [1989] The contribution of the input from the atmosphere to the contamination of the North Sea and the Dutch Wadden Sea. Report R89/349A, TNO, Delft, the Netherlands.

Williams R.M. [1982] A model for the dry deposition of particles to natural water surfaces. *Atmospheric Environment*, 16, 1933-1938.

scavenging rate during precipitation: $\Lambda = WR/H$, where W is an (empirical) scavenging ratio, R is the rain intensity and H the mixing height. An effective scavenging rate, Λ_{eff}, is estimated taking into account the intermittent nature of rain where it is assumed that the distribution of wet and dry periods over the source-receptor traject follows a Poisson distribution.

For Cd the initial particle size distribution (at the moment of emission), the mean dry deposition velocity, V_d, and mean scavenging rate, Λ_{eff}, are:

	<0.95 μm	0.95-4 μm	4-10 μm	10-20 μm	>20 μm
Cd (%)	42	33	14.5	5.9	4.6
V_d (ms^{-1})	0.00065	0.0025	0.0071	0.0132	0.067
Λ_{eff} (s^{-1})	$2.0\ 10^{-6}$	$1.5\ 10^{-5}$	$1.5\ 10^{-5}$	$1.5\ 10^{-5}$	$1.5\ 10^{-5}$

The uncertainty in the calculated concentrations and depositions, a) introduced by the modelling concepts of transport, diffusion and deposition are estimated to be about 30% including the meteorological variability; b) introduced by the choice of the particle size distribution of the emitted material at about 30-50% [*Baart et al*., 1995; *Van Jaarsveld et al.,* 1997].

References

Baart A.C. and H.S.M.A. Diederen [1991] Calculation of the atmospheric deposition of 29 contaminants to the Rhine catchment area. Report R91/219, TNO, Delft, the Netherlands.

Baart A.C., Berdowski J.J.M. and J.A. Van Jaarsveld [1995] Calculation of atmospheric deposition of contaminants on the North Sea. Report R95/138, TNO, Delft, the Netherlands.

Janssen A.J. and H.M. ten Brink [1985] Plume wash-out: modelling, calculation and validation. Report no 170, ECN, Petten, the Netherlands (in dutch).

Potma C.J.M. [1993] Description of the ECMWF/WMO Global Observational Data Set and associated data extraction and interpolation procedures. Report 722401001, RIVM, Bilthoven, the Netherlands.

Sehmel G.A. and W.J. Hodgson [1979] A model for prediction dry deposition of particles and gases to environmental surfaces. *A.I.Ch.E.Symposium Series,* 76**,** 196

Slinn W.G.N. [1977] Some approximations for the wet and dry removal of particles and gases from the atmosphere. *Water, Air Soil Pollut*, 7, 125-135.

Van den Hout K.D. (ed.) [1994] The impact of atmospheric deposition of non-acidifying compounds on the quality of European forest soils and the North Sea. Main report of the ESQUAD project. Report R93/329, TNO, Delft, the Netherlands.

Van Jaarsveld J.A. [1995] Modelling the long-term atmospheric behaviour of pollutants on various spatial scales. PH.D. thesis, University of Utrecht, the Netherlands.

Van Jaarsveld J.A., van Aalst R.M. and D. Onderdelinden [1986] Deposition of metals from the atmosphere into the North Sea: model calculations. Report 842015002, RIVM, Bilthoven, the Netherlands.

Van Jaarsveld, J.A., W.A.J. van Pul and F.A.A.M. de Leeuw. [1997] Modelling transport and deposition of persistent organic pollutants in the European region. *Atm. Env.* 31, 1011-1024.

Van Pul, W.A.J., W.A.S. Nijenhuis and F.A.A.M. de Leeuw [1998] Deposition of heavy metals to the Convention waters of OSPARCOM. Rivm report 722401016.

Warmenhoven J.P., Duiser J.A., de Leu L.Th. and C. Veldt [1989] The contribution of the input from the atmosphere to the contamination of the North Sea and the Dutch Wadden Sea. Report R89/349A, TNO, Delft, the Netherlands.

Williams R.M. [1982] A model for the dry deposition of particles to natural water surfaces. *Atmospheric Environment*, 16, 1933-1938.

Annex C

Maps of deposition and concentrations

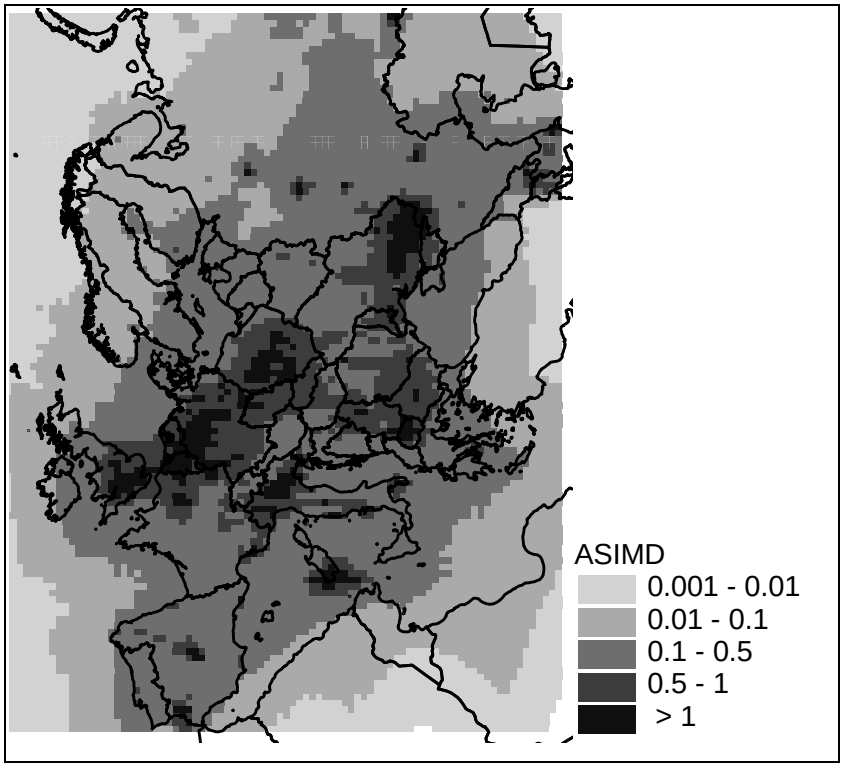

Figure C1. Cadmium concentrations in air for 1990 (ng/m^3). ASIMD model

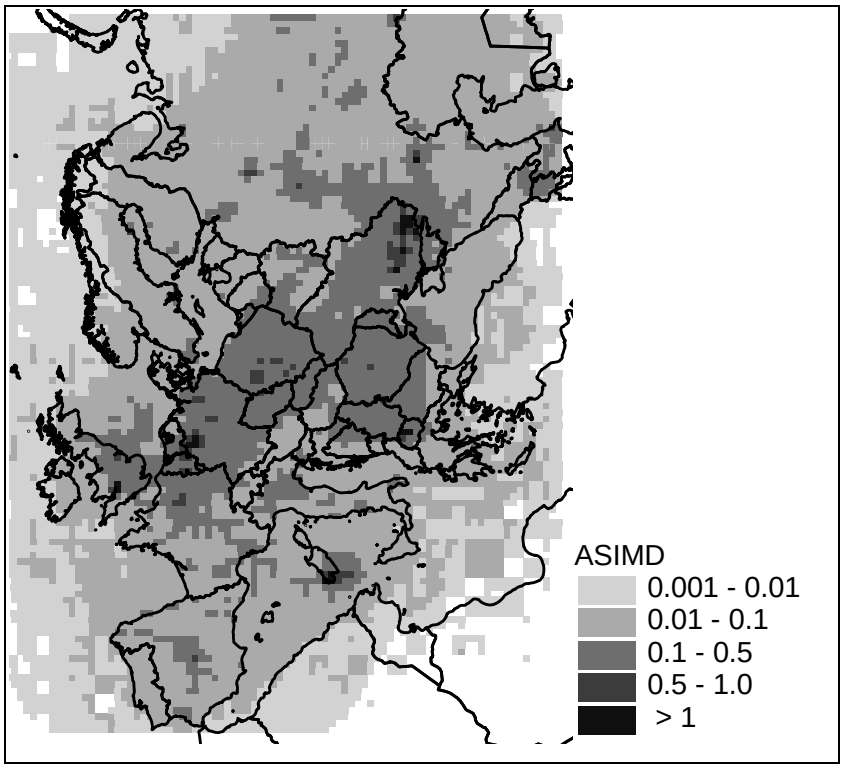

Figure C2. Cadmium concentrations in precipitation for 1990 (μg/l). ASIMD model

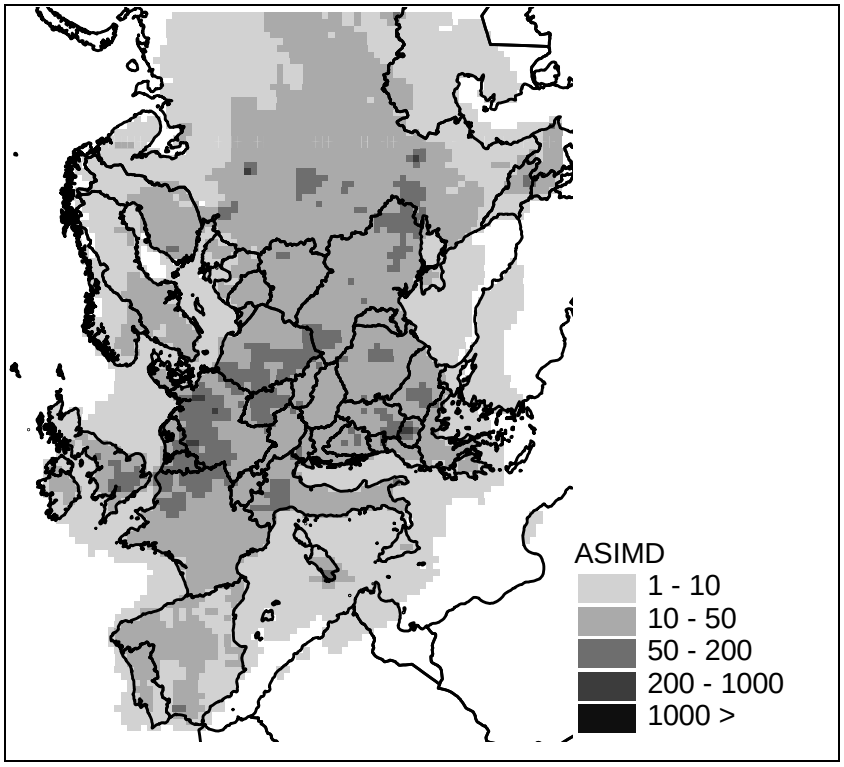

Figure C3. Cadmium dry deposition for 1990 ($\mu g/m^2$). ASIMD model.

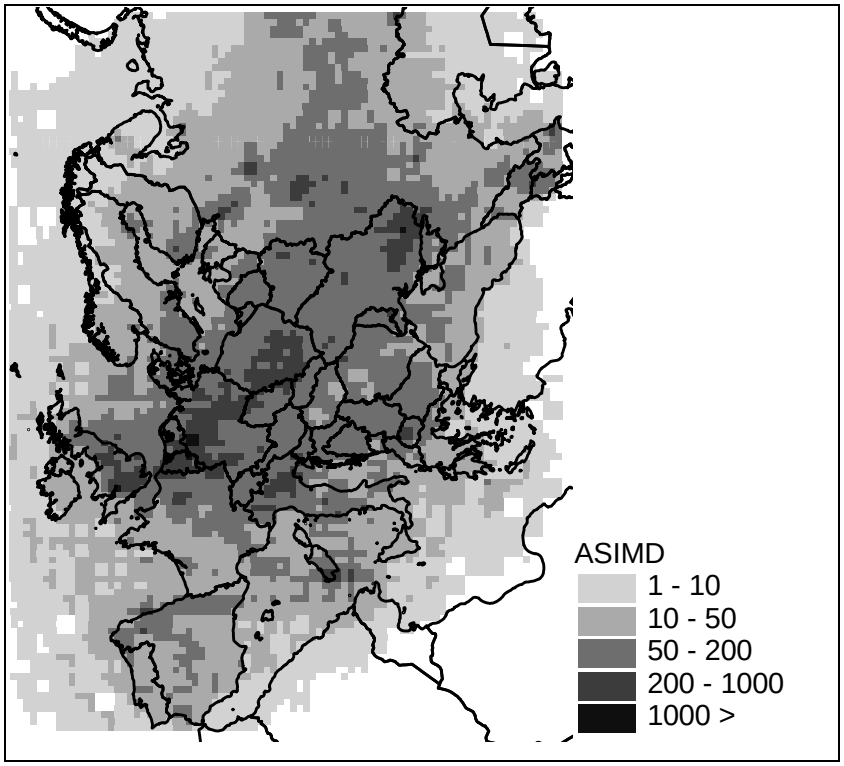

Figure C4. Cadmium wet deposition for 1990 ($\mu g/m^2$). ASIMD model.

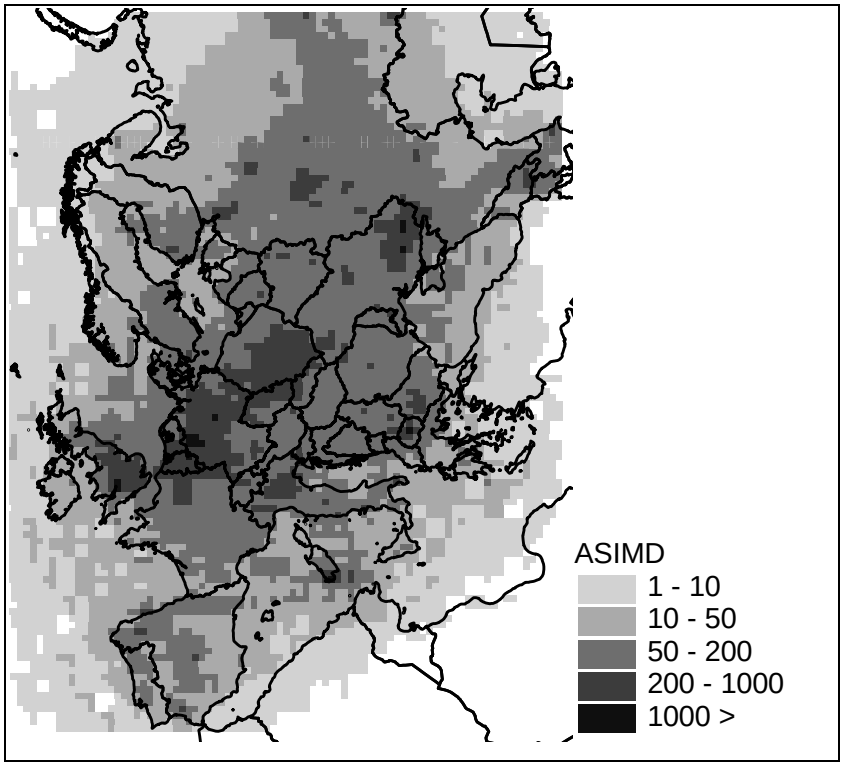

Figure C5. Cadmium total deposition for 1990 (μg/m^2).
ASIMD model.

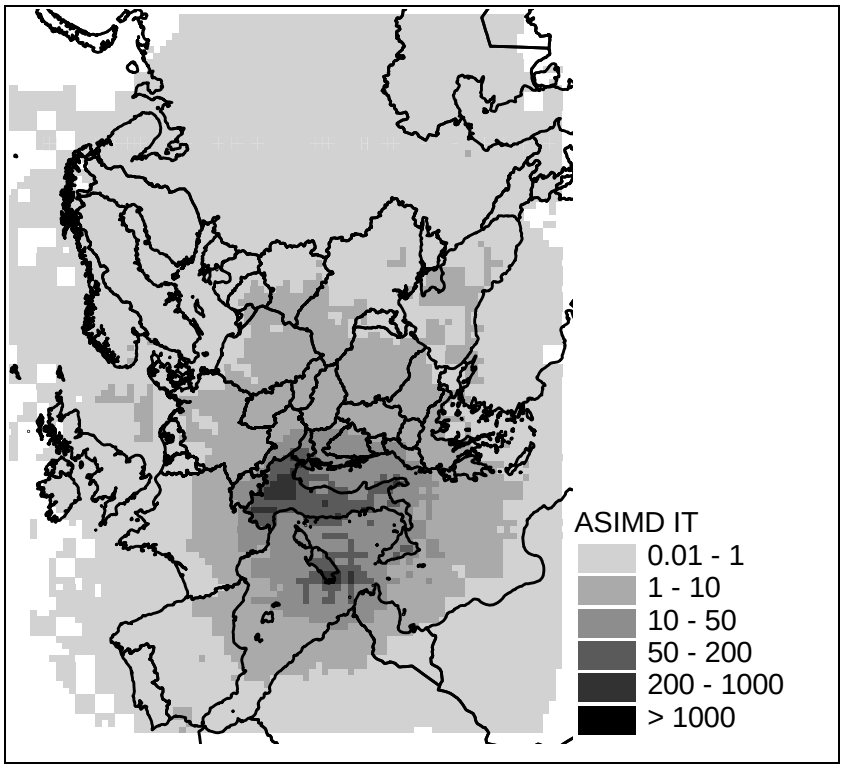

Figure C6. Cadmium total deposition from sources of Italy for 1990 (μg/m^2).
ASIMD model.

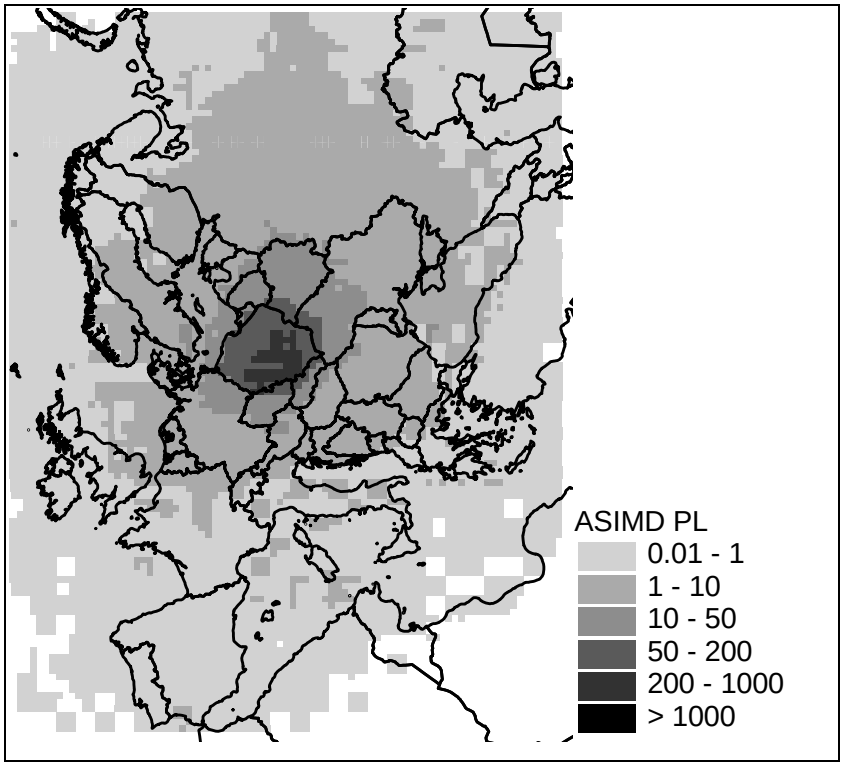

Figure C7. Cadmium total deposition from sources of Poland for 1990 (μg/m^2). ASIMD model.

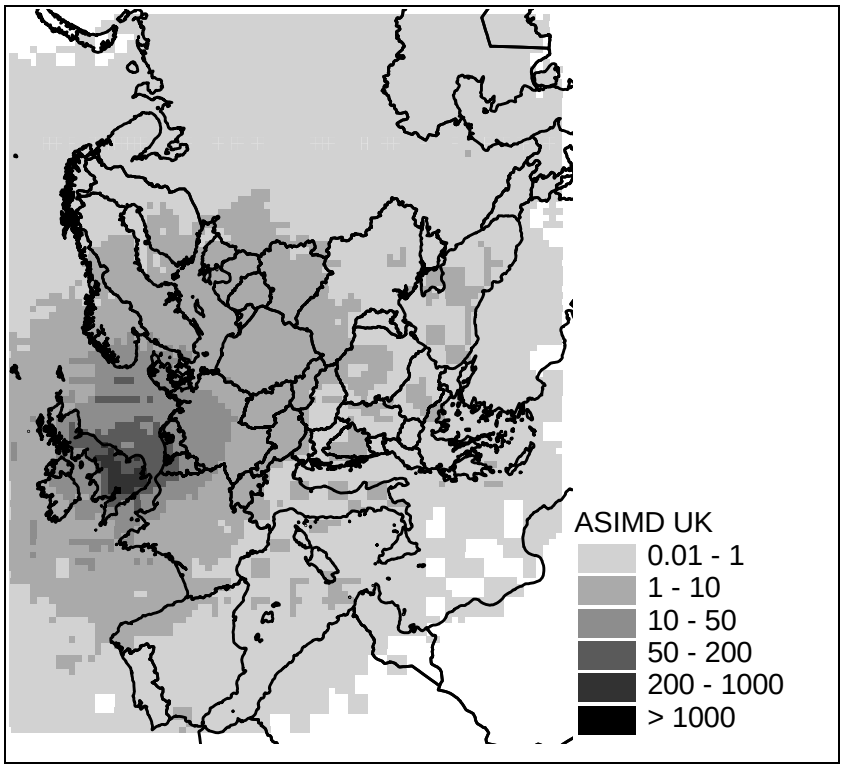

Figure C8. Cadmium total deposition from sources of United Kingdom for 1990 (μg/m^2). ASIMD model

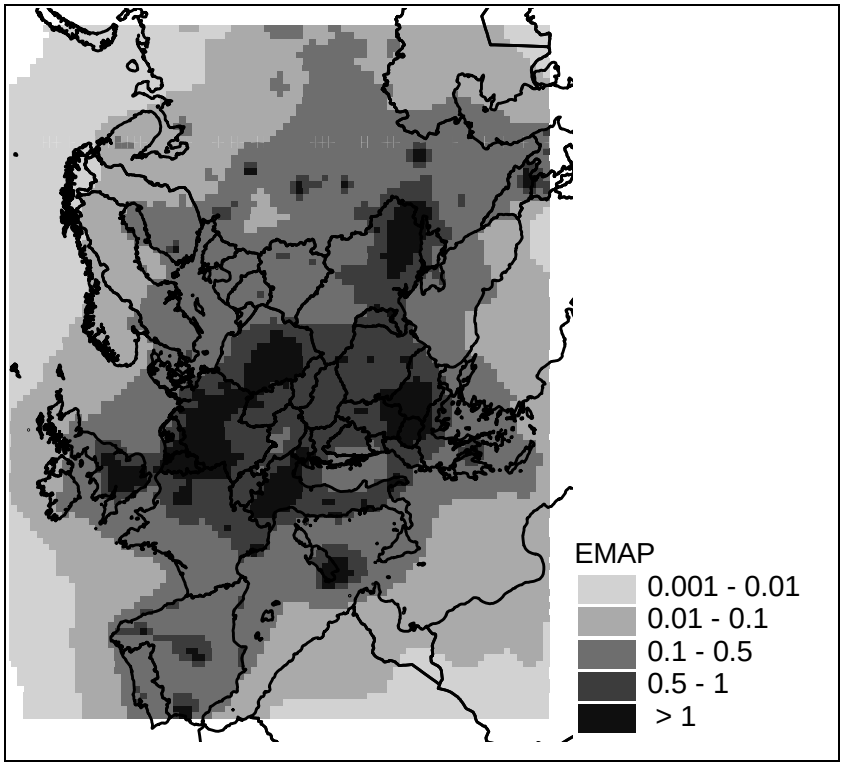

Figure C9. Cadmium concentrations in air for 1990 (ng/m^3). EMAP model.

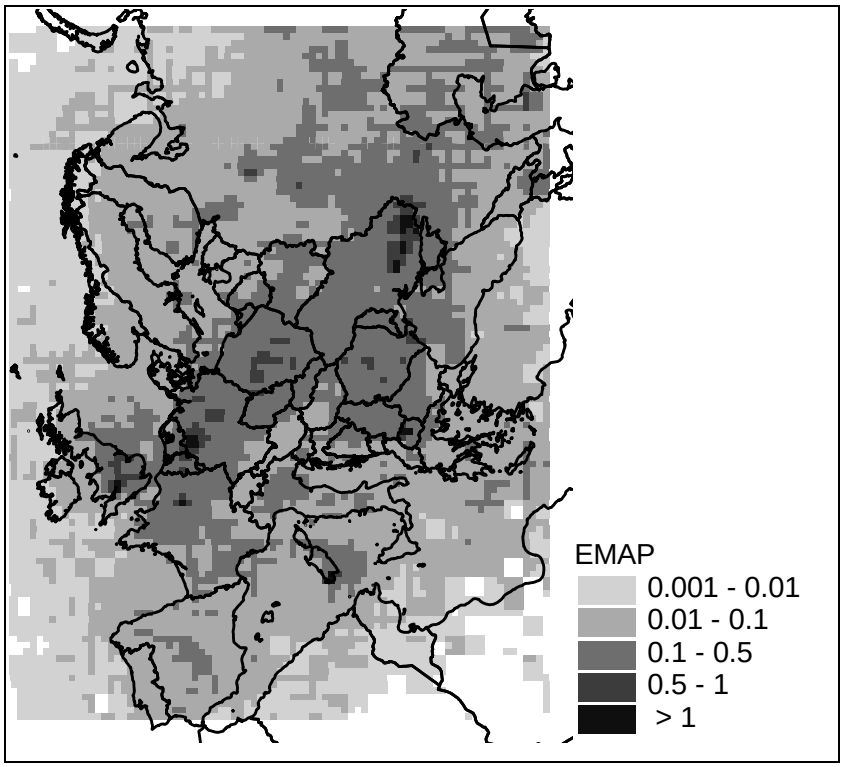

Figure C10. Cadmium concentrations in precipitation for 1990 (μg/l). EMAP model.

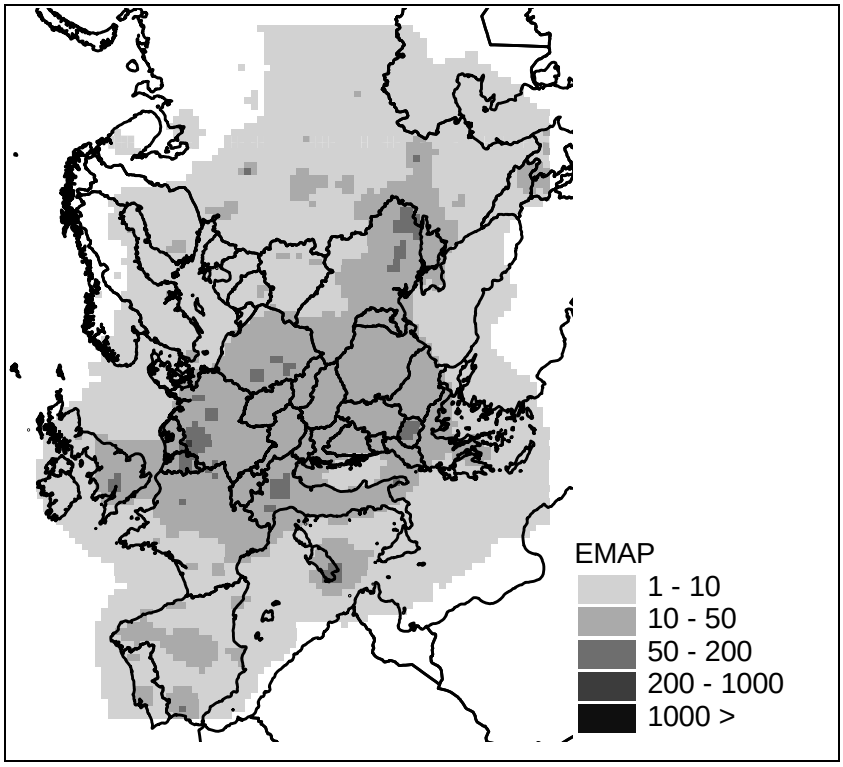

Figure C11. Cadmium dry deposition for 1990 ($\mu g/m^2$). EMAP model.

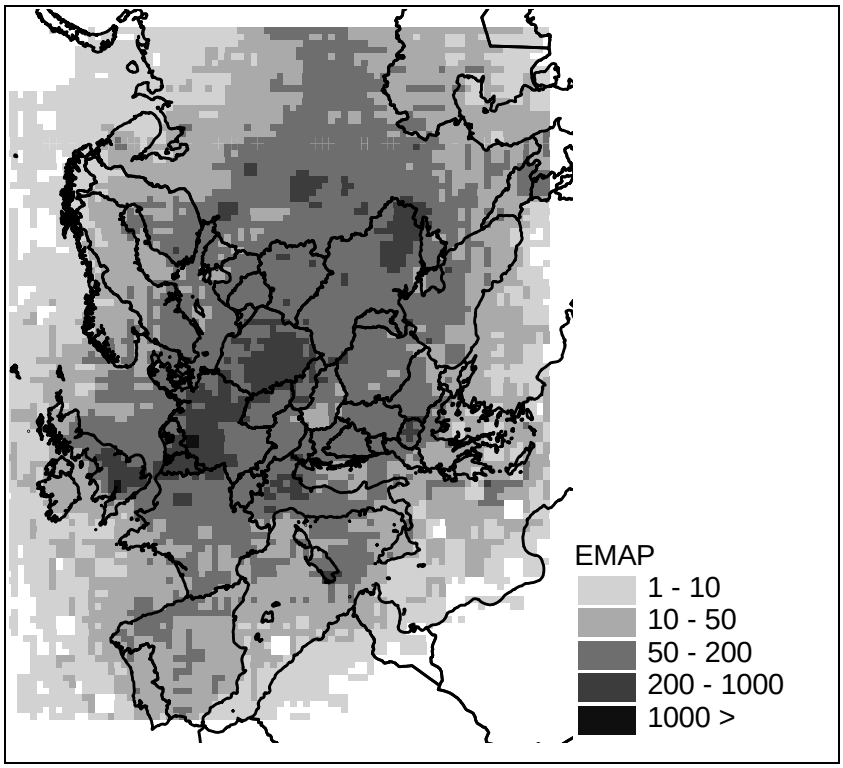

Figure C12. Cadmium wet deposition for 1990 ($\mu g/m^2$). EMAP model.

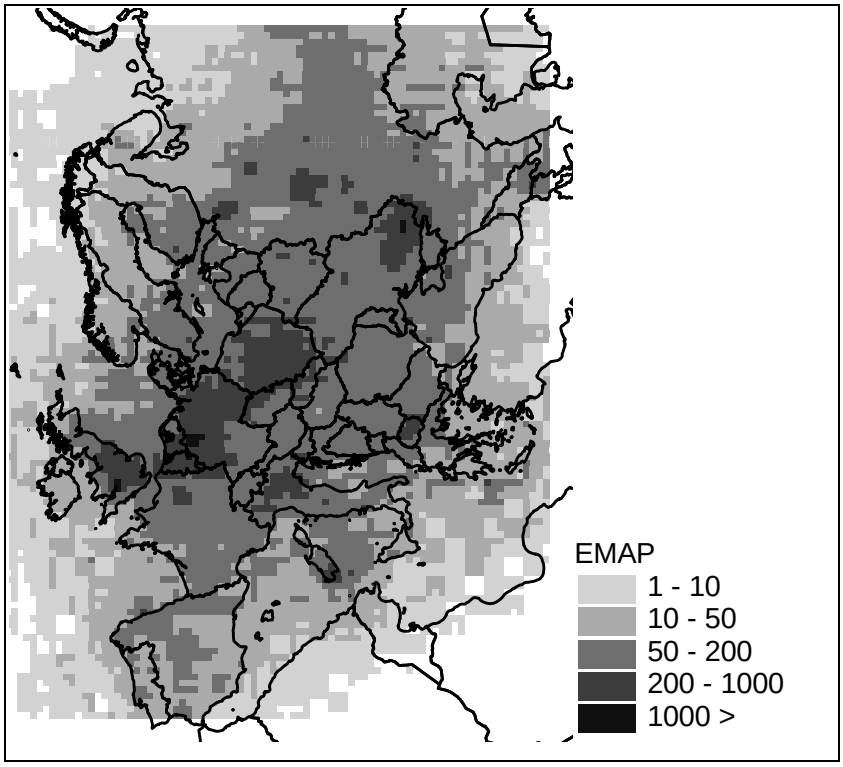

Figure C13. Cadmium total deposition for 1990 (μg/m^2). EMAP model.

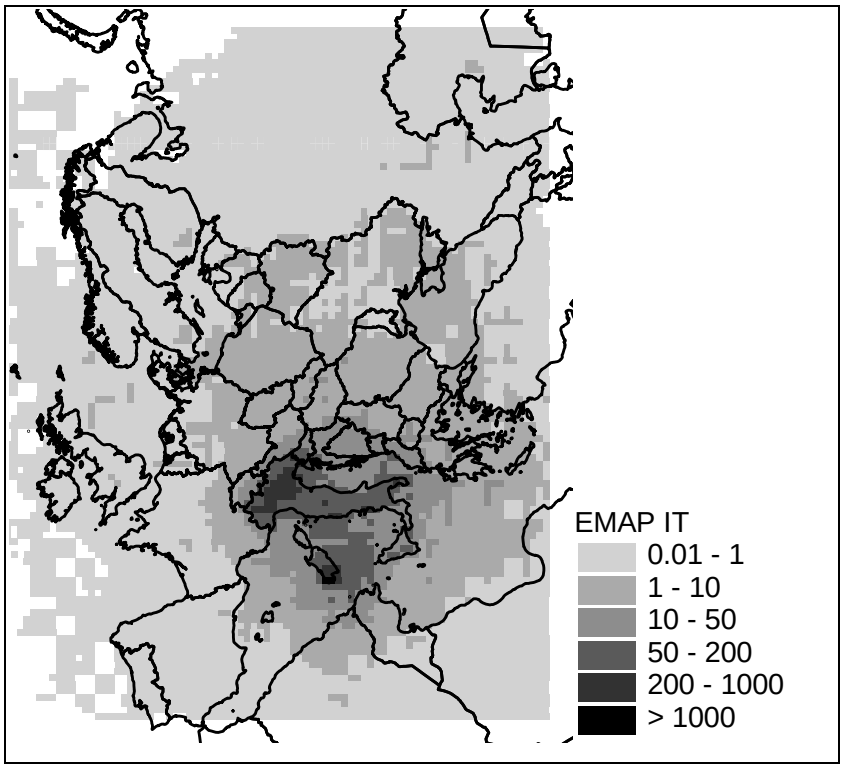

Figure C14. Cadmium total deposition from sources of Italy for 1990 (μg/m^2). EMAP model.

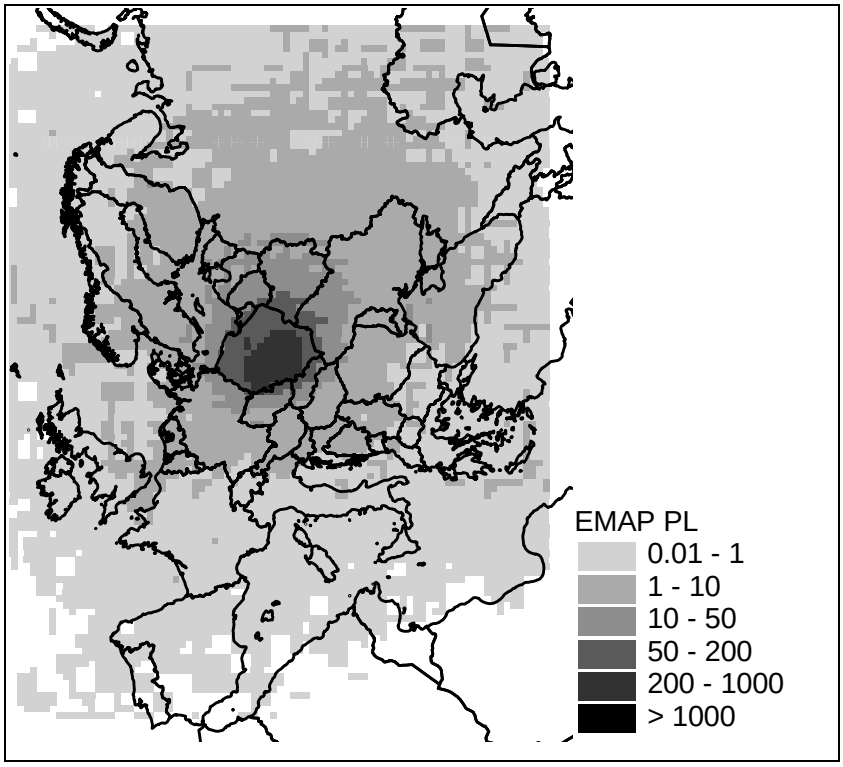

Figure C15. Cadmium total deposition from sources of Poland for 1990 (μg/m^2). EMAP model.

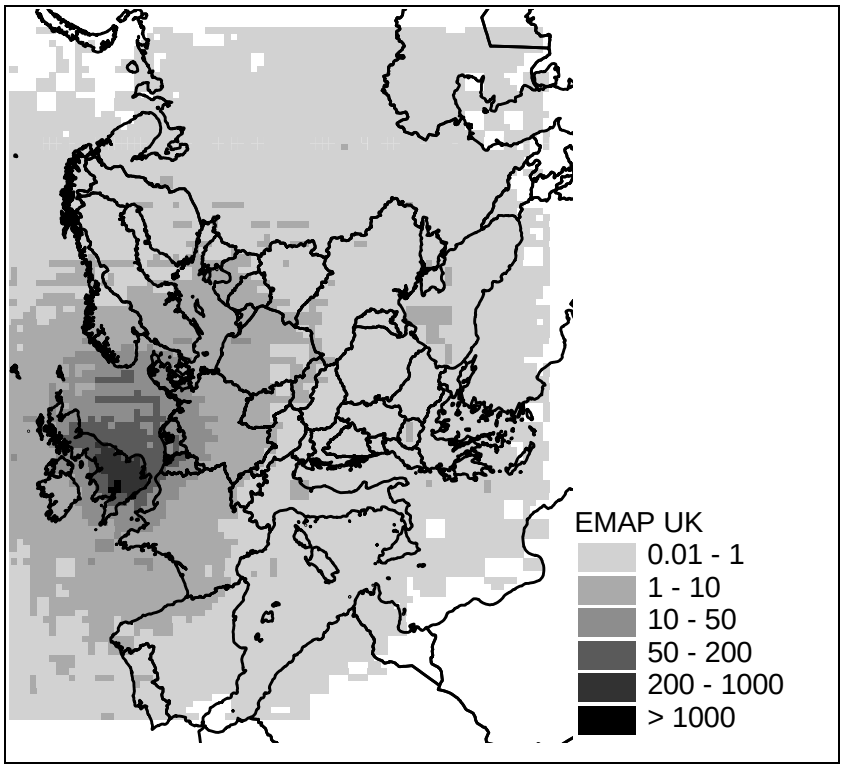

Figure C16. Cadmium total deposition from sources of United Kingdom for 1990 (μg/m^2). EMAP model.

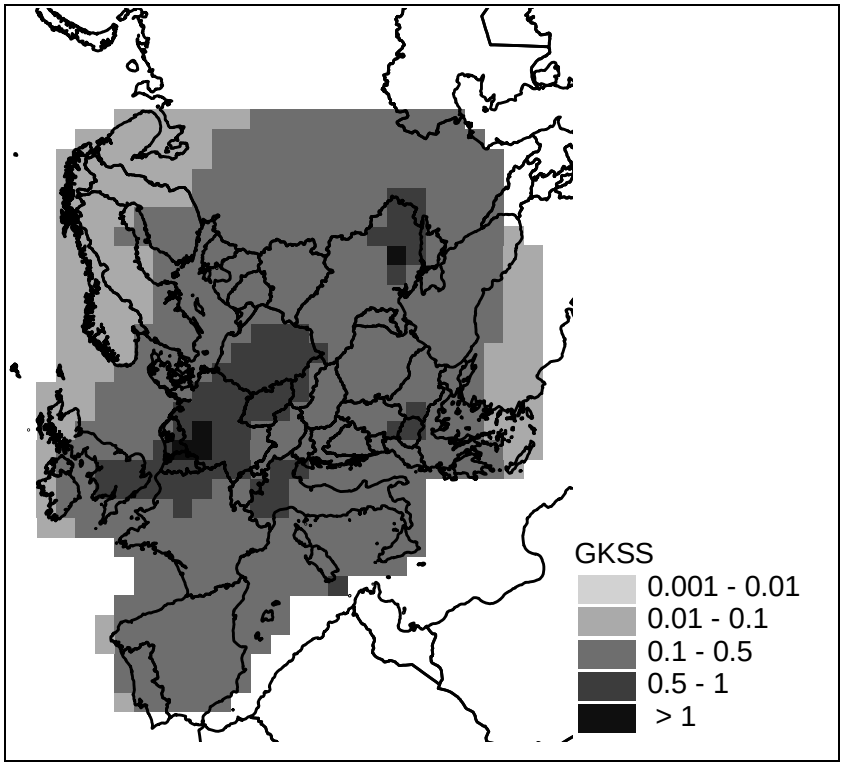

Figure C17. Cadmium concentrations in air for 1990 (ng/m^3). GKSS model.

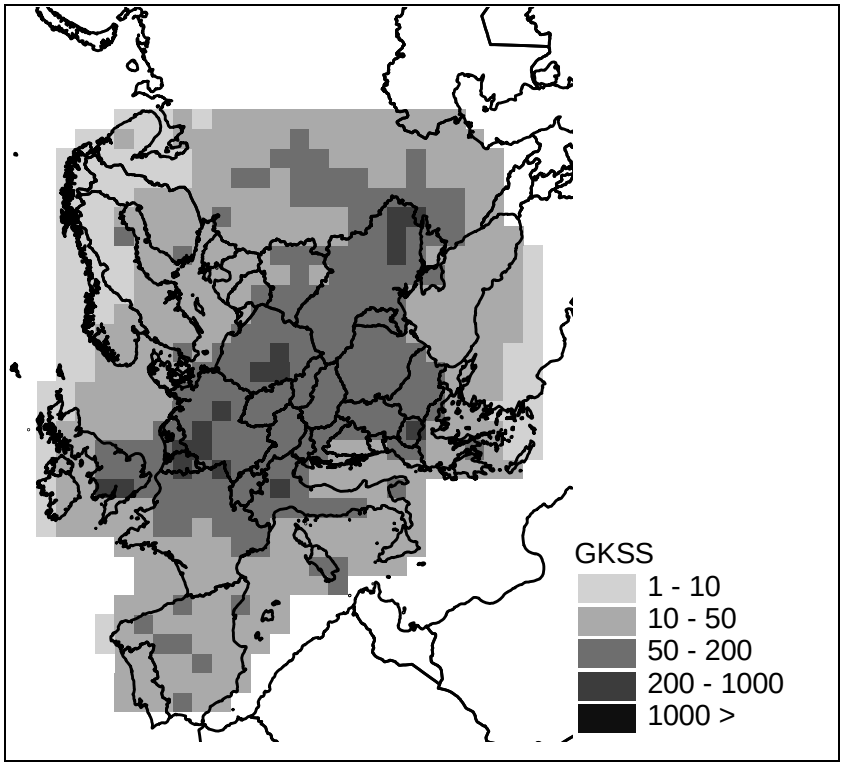

Figure C18. Cadmium dry deposition for 1990 (μg/m^2). GKSS model.

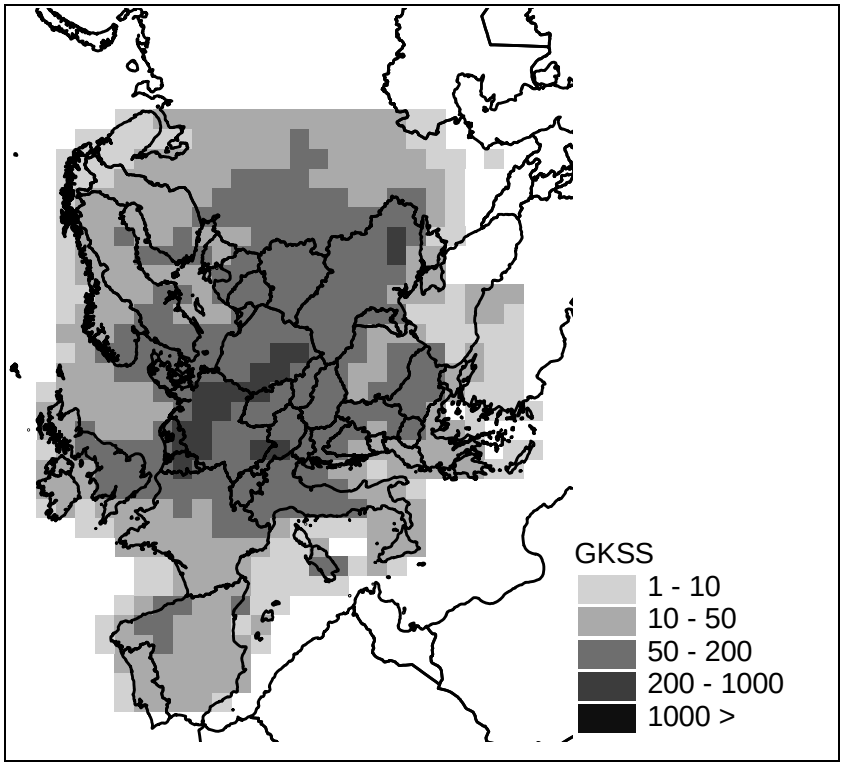

Figure C19. Cadmium wet deposition for 1990 ($\mu g/m^2$). GKSS model.

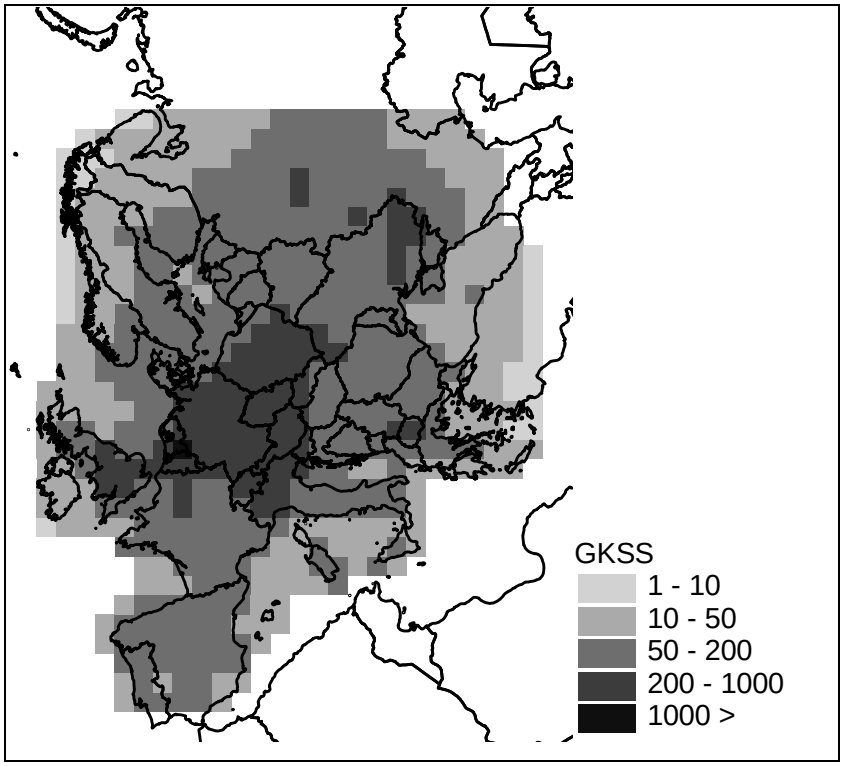

Figure C20. Cadmium total deposition for 1990 ($\mu g/m^2$). GKSS model.

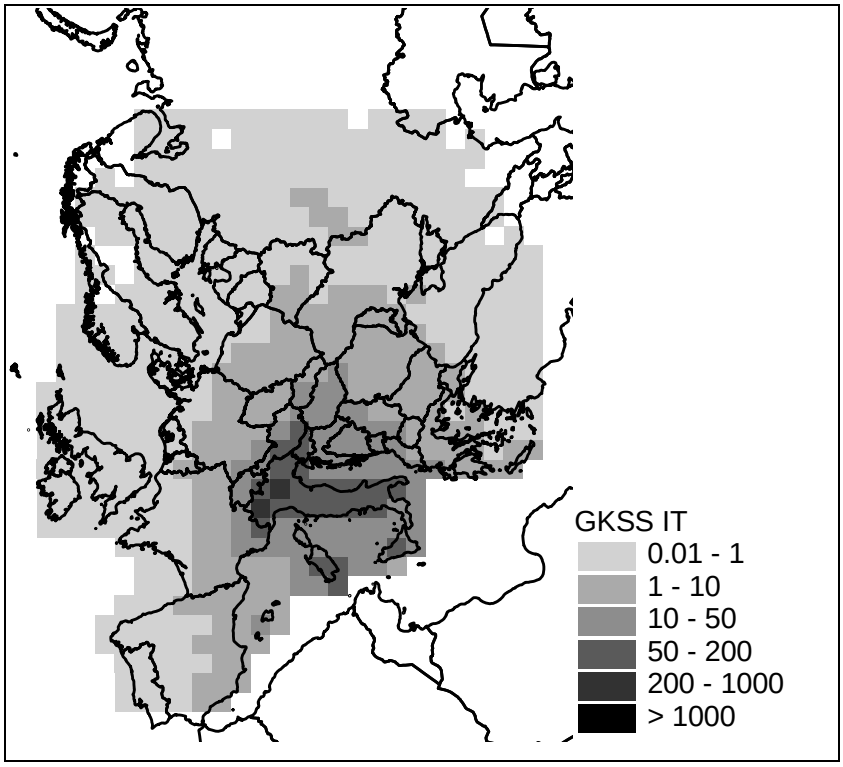

Figure C21. Cadmium total deposition from sources of Italy for 1990 (μg/m^2). GKSS model.

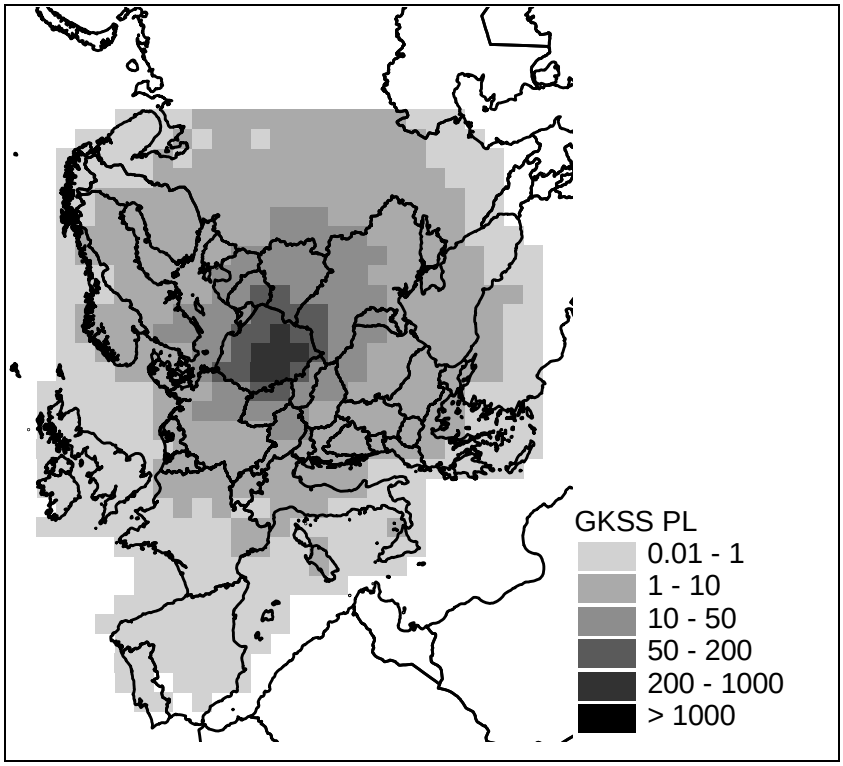

Figure C22. Cadmium total deposition from sources of Poland for 1990 (μg/m^2). GKSS model.

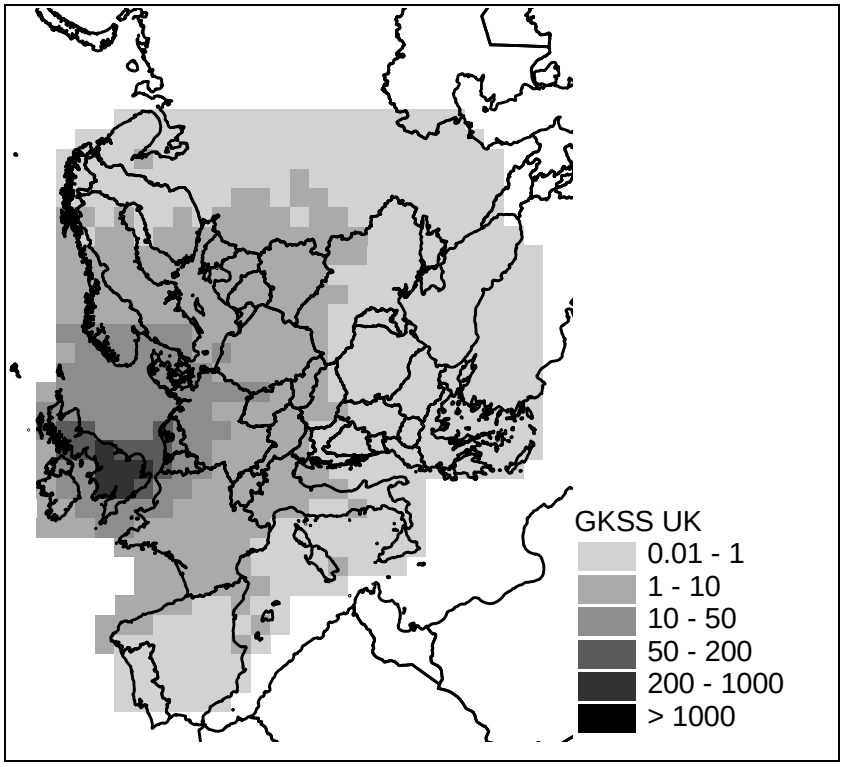

Figure C23. Cadmium total deposition from sources of United Kingdom for 1990 ($\mu g/m^2$). GKSS model.

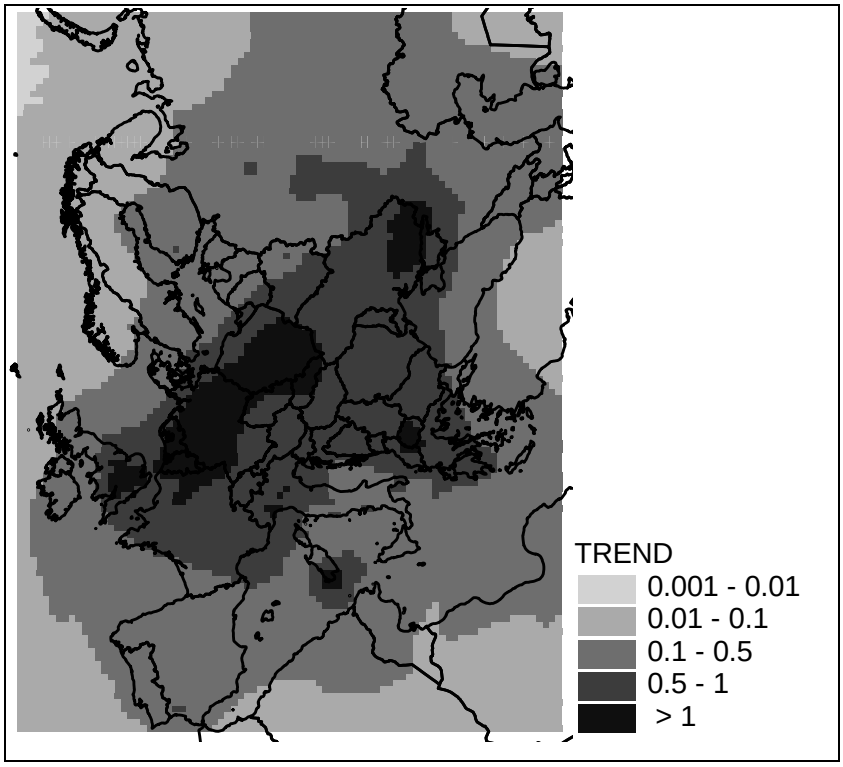

Figure C24. Cadmium concentrations in air for 1990 (ng/m^3). TREND model.

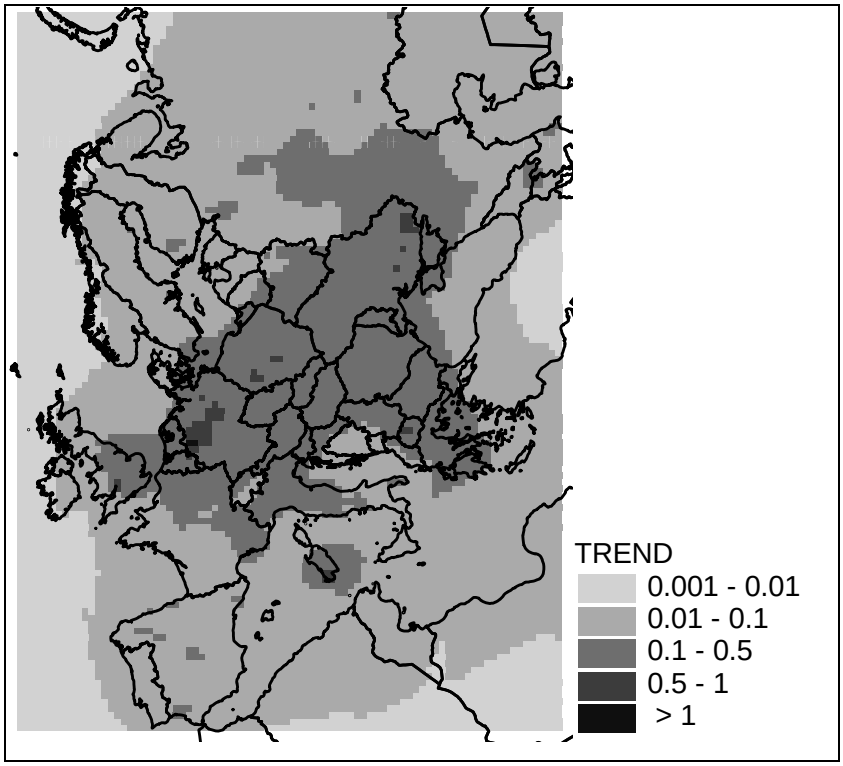

Figure C25. Cadmium concentrations in precipitation for 1990 (μg/l). TREND model.

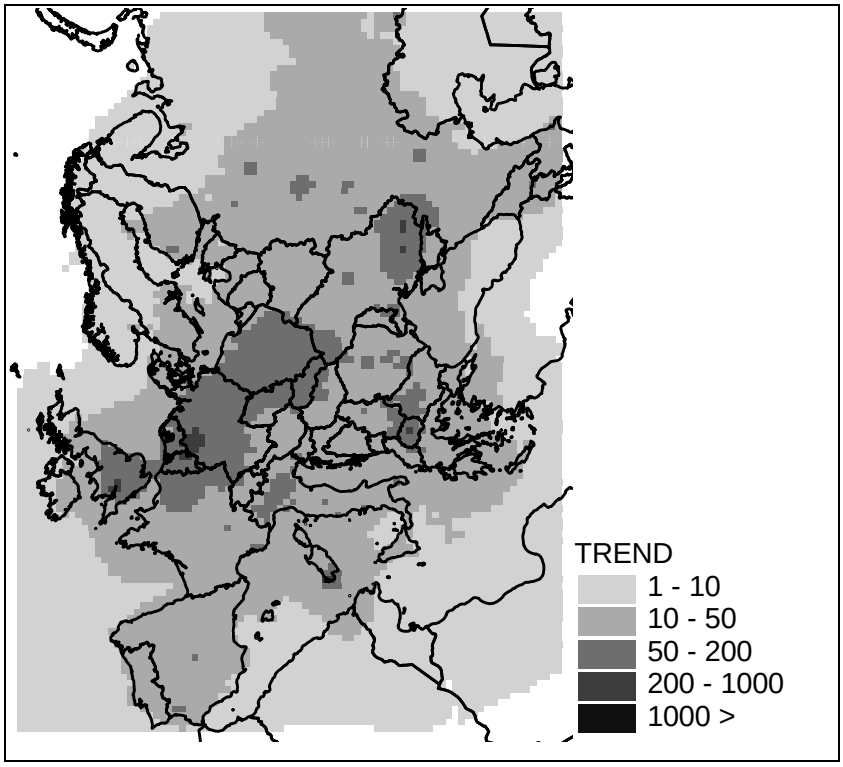

Figure C26. Cadmium dry deposition for 1990 (μg/m^2). TREND model.

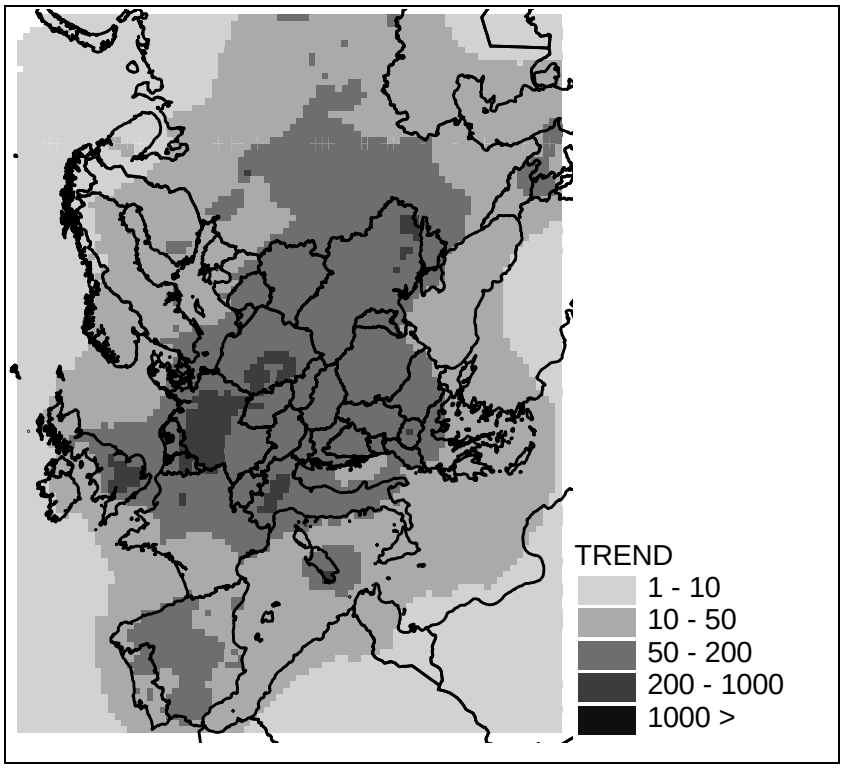

Figure C27. Cadmium wet deposition for 1990 (μg/m^2). TREND model.

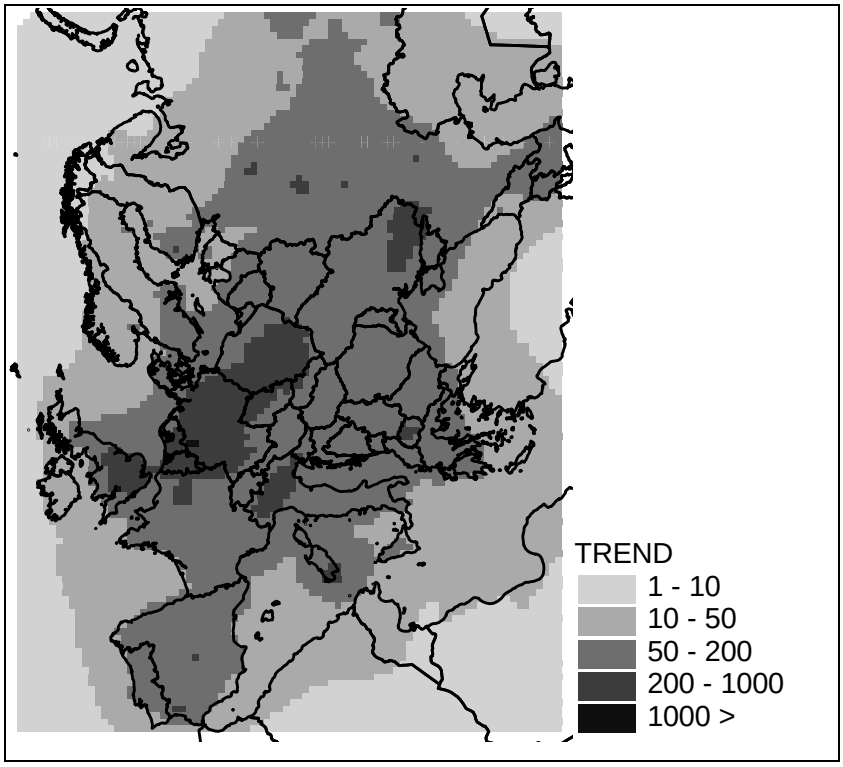

Figure C28. Cadmium total deposition for 1990 (μg/m^2). TREND model.

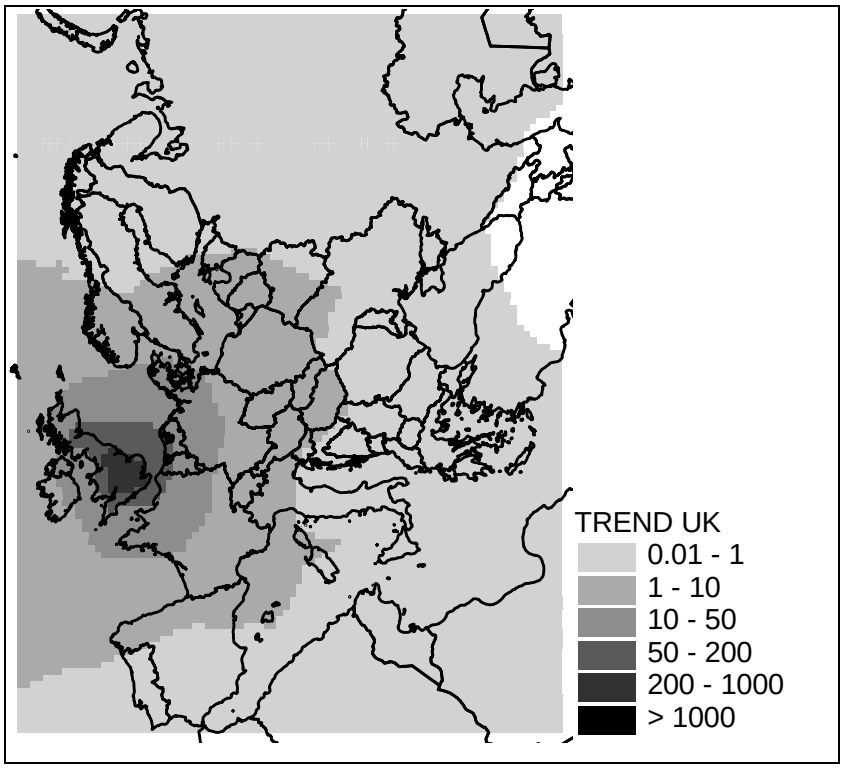

Figure C29. Cadmium total deposition from sources of United Kingdom for 1990 (μg/m^2). TREND model.

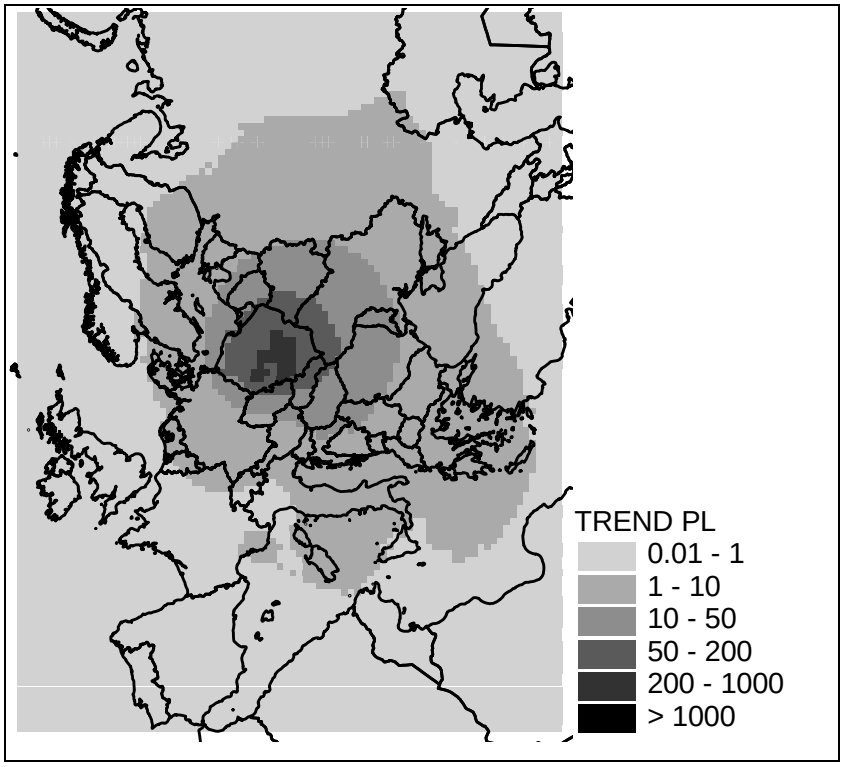

Figure C30. Cadmium total deposition from sources of Poland for 1990 (μg/m^2). TREND model.

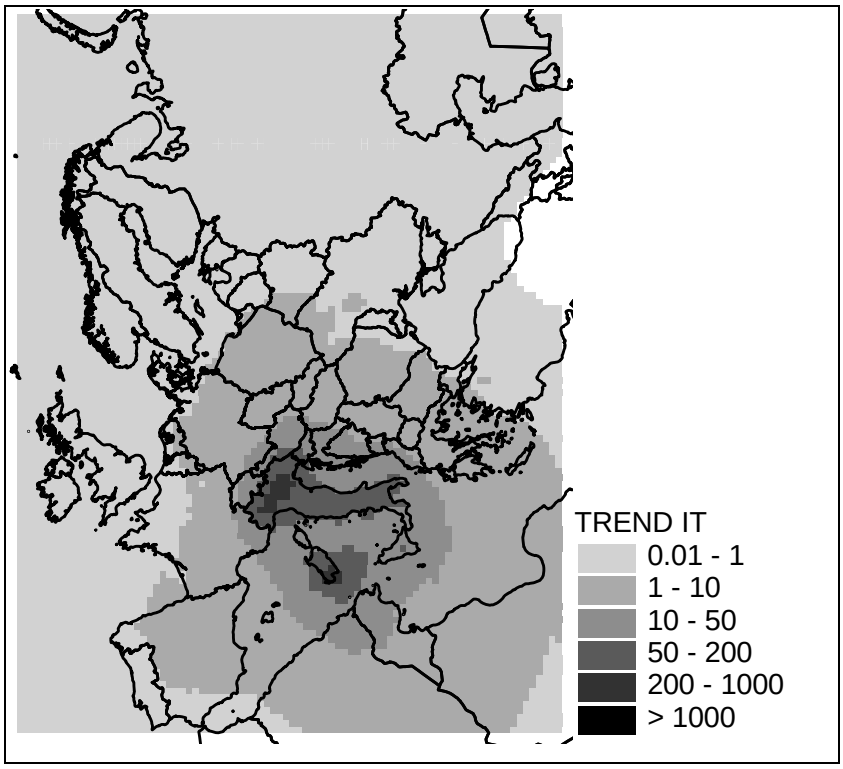

Figure C31. Cadmium total deposition from sources of Italy for 1990 (μg/m^2). TREND model.

About EMEP/MSC-E participation in ATMES-II

Margarita Pekar

Introduction

Large-scale field experiments concerned with environmental pollution are major events for the scientific community involved in the problem. Apart from the direct participation of a wide range of investigators in these experiments, database is used for the verification of pollution transport models. ETEX (European Tracer Experiment) was the last experiment of such kind in which besides “Dry runs” two releases of passive pollutants dispersed within the scope of Europe were carried out in October and November of 1994. The experiment was aimed at measuring pollutant concentrations at a wide network of sampling sites required for the verification of prognostic models operating in real time. Nearly two years later ATMES-II (Atmospheric Transport Model Evaluation Study II) was carried out which presumed to compare the results of long-range transport model results with measurements of the ETEX first release. In some sense ATMES-II is a continuation of ATMES experiment performed in 1992 which was aimed at comparing the results of long-range transport models with observations of Cs^{137} and I^{131} concentrations and depositions after Chernobyl accident. MSC-E (Meteorological Synthesizing Centre-East) took part in both ATMES projects. Our models are oriented on the solution of problems different from those of emergency response characterized by a point source and relatively short period of the impact. MSC-E is engaged in modelling of heavy metals (Pb, Cd, Hg) and POPs within European region with multiple sources of continuous emissions and minimum time of integration of 1 year. Comparison of different approaches to modelling of the long-range dispersions encourage further model development. In any case we paid attention to the importance of reliable meteorological data, correctness of time and spatial interpolation of the data, wind field mass consistency and other factors discussed in ETEX and ATMES-II proceedings.

In this paper it is intended to present concise descriptions of the models participated in ATMES-II project in the order of their ranking according to global statistical indices, to evaluate shortcomings of our model and to determine steps for their elimination.

The information used was taken from: S.Mosca, R.Bianconi, R.Bellasio, G.Grasiani, W.Klug, ATMES-II - Evaluation of Long-Range Dispersion Models using data of the 1st ETEX release. Luxembourg: Office of Official Publications of the European Communities, 1998.

Experiment conditions

ETEX first release started on 23 Oct. 1994, 1600 UTC and ended on 24 Oct. 1994, 0350 UTC.

The source was located at Monterfil (2^o 00' 30" W; 48^o 03' 30" N; 90 m asl) in Bretagne, France.

340 kg of Perfluoro-Methyl-Cyclo-Hexane (PMCH) was being released during 12 hours with speed 7.95 g/s.

The sampling network consisted of 168 sites located in 17 European countries to the east of the release point. Air samples were taken every 3 hours during 72 hours.

49 models participated in ATMES-II. 35 models (numerical codes: 101-135) used meteorological data of ECMWF (European Centre for Medium range Weather Forecast), the models which used non-ECMEF data have numerical code 201-214.

ECMWF meteodata have spatial resolution 0.5^o x 0.5^o, only 31 levels along the vertical, 14 levels below 500 hPa and temporal resolution - 6 hours.

Statistical methodology

Statistical analysis was performed on the basis of predicted and measured three-hour-averaged tracer concentrations using 30 values only for each sampling site (with allowance for the experiment duration of 90 hours). The global analysis was made - the total set of concentrations M (x_i, t_j) and P(x_i, t_j) is considered, here M (x_i, t_j) and P(x_i, t_j) are measured and predicted concentrations in point x_i at time t_j. Hereinafter pairs of concentrations will be designated as (M_i P_i) where i is the pair index. Space analysis - the concentration over the whole region is considered in a specific point of time; time analysis - concentration in a specific point is considered for the whole period of the experiment.

Below statistical characteristics used for the comparison of measured and predicted values are enumerated: Scatter diagram, *FOEX*, $FA\alpha$:

$$FOEX = \left[\frac{N(P_i > M_i)}{N} - 0.5 \right] \cdot 100 ,$$

Here N - number of pairs; $FA\alpha$ - fraction of points on the scatter diagram falling on the band: $(y - y_0) = (x - x_0) \pm \alpha$

Bias:

$$B = \frac{1}{N}\sum_i (P_i - M_i)\,.$$

Geometric mean bias:

$$MG = \exp\left[\frac{1}{N}\sum_i \ln\left(\frac{M_i}{P_i}\right)\right].$$

NMSE (Normalized mean Square Error):

$$NMSE = \frac{1}{N}\sum_i \frac{(P_i - M_i)^2}{\overline{P}\,\overline{M}}; \quad \overline{P} = \frac{1}{N}\sum_i P_i; \quad \overline{M} = \frac{1}{N}\sum_i M_i\ .$$

Geometrical mean variance:

$$VG = \exp\left[\frac{1}{N}\sum_i \left(\ln\frac{M_i}{P_i}\right)^2\right]$$

Pearson's correlation coefficient:

$$P_{corr} = \frac{\sum_i \left(\ln M_i - \overline{\ln M}\right)\left(\ln P_i - \overline{\ln P}\right)}{\left(\sum_i \left(\ln M_i - \overline{\ln M}\right)^2\right)^{1/2}\left(\sum_i \left(\ln P_i - \overline{\ln P}\right)^2\right)^{1/2}}$$

where: $\overline{\ln P} = \frac{1}{N}\sum_i \ln P_i; \quad \overline{\ln M} = \frac{1}{N}\sum_i \ln M_i;$

Box plot and percentiles: for cumulative distributions box plot is constructed in which 25th, 50th, 75th percentiles are indicated.

Kolmogorov-Smirnov parameter: assessment of the difference between cumulative distributions of the observed and predicted concentrations.

$KS = N$ Max |prob ($P(x_l)$) - prob ($M(x_l)$)|,

where prob ($P(x_l)$) and prob ($M(x_l)$) - cumulative frequencies with the probability not more than x_l of the appearance of predicted and measured values.

Figure of Merit in Space (FMS) equals the percentage of overlapping of the measured and predicted areas at a fixed time, for fixed concentration level.

Figure of Merit in time (FMT) is calculated for a definite point x for the whole period of time and it is the histogram of overlapping concentrations measured and predicted at each time interval.

Integrated concentration or doze is determined in *x* point for *N* time periods:

$$I_N(x) = \sum_{j=1}^{N} M(\bar{x}_i t_j)(t_j - t_{j-1}) .$$

All the listed statistical estimates were carried out by Team Group for each model and they are presented in [1]. It gave a possibility to make a thorough evaluation of a model quality and to rank models versus their quality.

Model ranking

The statistical analysis results of models outcome are described in [1]. There is ranking of the models which used ECMWF meteorological data, then come the models which used another meteorological data and the integrated table presenting ranking of all 49 models participated in ATMES-II project. For the sequential consideration of the models we will use the integrated table 1 with the same rank designations, i.e. each model is indicated by the same ordinal number being a model rank, then the authors of the model are presented, then come the model number and corresponding ordinal numbers among 35 models the same as in [1]. When a model tested with different meteorological data or in deferent modifications considered as different models is mentioned for the first time, all variants of the models with their ranks are listed. For example, the model by *H.Glaab*, *B.Fay*, *I.Jacobson* has 3 realizations enumerated as models 107, 106, 203; among them model 107 has rank 1 corresponding to designation 1/49 and its rank among 35 models is also presented - 1/35. Model 106 has rank 42 and it will be mentioned on its 42^{d} place and model 203 (non-ECMWF data) has rank 4 among 14 models, 4/14, and rank 4 among 49 models, 4/49. Table 2 demonstrates ranking of models, which used ECMWF data. Table 3 presents two-dimensional distribution of the models according to their ranks and simulation methods (Lagrangian particle method, particles with transition to puffs; particles along the vertical, puffs along the horizontal; particles with transition to Eulerian description; Lagrangian puffs, puffs with the transition to Eulerian description and finally pure Eulerian description). Table 4 presents a similar distribution for selected 35 models, which used ECMWF data. In publication [*Mosca et al.*, 1998] lacks the description of some models: 124, 125, 126, 129.

Table 1. Model ranking according to the analysis results [*Mosca et al.*, 1998]

№	Authors, Country, Organization	Models	Ranks
1	H.Glaab, B.Fay, I.Jacobsen ***D***	107	1/35 1/49
	German Weather Service, DWD	106	30/35 42/49
		203	4/14 4/49
2	M.Monfort ***F*** French Institute for Nuclear Protection and Safety, IPSN	111	2/35 2/49
3	R.H.Maryon and D.B.Ryall ***UK***	209	1/14 3/49
	Meteorological Office, Metoff	210	2/14 6/49
		119	11/35 21/49
4	H.Glaab, B.Fay, I.Jacobsen ***D*** German Weather Service, DWD	203	4/14 4/49
5	D.Anfossi ***I*** National Research Council, CNR	114	5/35 5/49
6	R.H.Maryon, D.B.Ryall ***UK*** Meteorological Office, Metoff	210	2/14 6/49
7	J.Saltbones, A.Foss, J.Bartnicki ***N***	131	3/35 7/49
	Norwegian Meteorological Institute, DNMI	213	5/14 11/49
8	L.Robertson, J.Langner, C.Persson, A.Ullerstig ***S***	208	3/14 8/49
	Swedish Meteorological and Hydrological Institute, SMHI	128	9/35 15/49
9	H.Yamazawa, M.Chino, H.Nagai, A.Furuno ***J***	115	4/35 9/49
	Japan Atomic Energy Research Institute JAERI		
10	A.Stohl ***A*** Institute of Meteorology and Physics,	101	7/35 10/49
	University of Wien, IMP		
11	J.Saltbones, A.Foss, J.Bartnicki ***N***	213	5/14 11/49
	Norwegian Meteorological Institute, DNMI		
12	J.S.Nasstrom, T.C.Pace ***USA*** Lawrence Livermore Nation.	127	6/35 12/49
	Laboratories, LLNL		
13	J.Brandt, J.Christensen, A.Ebel, H.Elbern, H.Jacobs,	204	6/14 13/49
	M.Memmesheimer, T.Mikkelsen, S.Thykier-Nielsen and Z.Zlatev ***D/DK***	108	19/35 28/49
	National Environment Research Institute/Risoe	109	16/35 20/49
	Nat.Lab./Univ.of Cologne, NERI		
14	D.Wendum ***F*** French Electricity EDF	112	8/35 14/49
15	L.Robertson, J.Langner, C.Persson, A.Ullerstig ***S***	128	9/35 15/49
	Swedish Meteorological and Hydrological Institute, SMHI		
16	J.H.Sørensen, A.Rasmussen ***DK***	205	7/14 16/49
	Danish Meteorological Institute, DMI	110	22/35 31/49
17	T.Iwasaki, T.Maki ***J***	134	10/35 17/49
	Japan Meteorological Agency, JMA	133	26/35 40/49
18	F.Desiato ***I*** National Agency for Environment, ANPA	113	12/35 18/49
19	L.Thaning ***S*** Defence Research Establishment, FOA	118	13/35 19/49
20	J.Brandt, J.Christensen, A.Ebel, H.Elbern, H.Jacobs,	109	16/35 20/49
	M.Memmesheimer, T.Mikkelsen, S.Thykier-Nielsen and Z.Zlatev ***D/DK***		
	National Environment Research Institute/Risoe Nat.Lab./Univ.of		
	Cologne, NERI		
21	R.H.Maryon, D.B.Ryall ***UK*** Meteorological Office, Metoff	119	11/35 21/49
22	M.Pekar ***RU***	135	14/35 22/49
	Meteorological Synthesizing Centre East, MSC-E	214	9/14 29/49
23	**** NL*** Royal Dutch Meteorological Institute KNMI	124	15/35 23/49
24	J.Sato, H.Sasaki, K.Adachi ***J***	116	18/35 24/49
	Meteorological Research Institute, MRI	207	11/14 34/49
25	**** NL*** Royal Dutch Meteorological Institute KNMI	125	17/35 25/49
26	B.J.Stunder, B..Draxler, D.Hess ***USA***	211	8/14 26/49

	National Oceanic and Atmospheric Administration, NOAA	120	27/35 39/49
27	R.I.Sykes and R.S.Gabruk ***USA*** ARAP Group of Titan Research and Technology, ARAP	121	20/35 27/49
28	J.Brandt, J.Christensen, A.Ebel, H.Elbern, H.Jacobs, M.Memmesheimer, T.Mikkelsen, S.Thykier-Nielsen and Z.Zlatev ***D/DK*** National Environment Research Institute/Risoe Nat.Lab./Univ.of Cologne, NERI	108	19/35 28/49
29	M.Pekar ***RU*** Meteorological Synthesizing Centre East, MSC-E	214	9/14 29/49
30	G.O.Hess, R.R.Draxler ***AUS*** Bureau of Meteorological Research Centre, BMRC	102 201	21/35 30/49 10/14 32/49
31	J.H.Sørensen, A.Rasmussen ***DK*** Danish Meteorological Institute, DMI	110	22/35 31/49
32	G.O.Hess, R.R.Draxler ***AUS*** Bureau of Meteorol. Research Centre, BMRC	201	10/14 32/49
33	R.D'Amours ***CND*** Canadian Meteorological Centre, CMC	202 105	12/14 33/49 23/35 35/49
34	J.Sato, H.Sasaki, K.Adachi ***J*** Meteorological Research Institute, MRI	207	11/14 34/49
35	R.D'Amours ***CND*** Canadian Meteorological Centre, CMC	105	23/35 35/49
36	F.Bompay ***F*** Meteo-France, Meteo	123 206	25/35 36/49 13/14 43/49
37	D.Syrakov and M.Prodanova ***BG*** National Institute for Meteorology and Hydrology, NIMH-BG	104 103	24/35 37/49 28/35 38/49
38	D.Syrakov and M.Prodanova ***BG*** National Institute for Meteorology and Hydrology, NIMH-BG	103	28/35 38/49
39	B.J.Stunder, B.Draxler, D.Hess ***USA*** National Oceanic and Atmospheric Administration, NOAA	120	27/35 39/49
40	T.Iwasaki, T.Maki ***J*** Japan Meteorological Agency, JMA	133	26/35 40/49
41	* ***NL*** Royal Dutch Meteorological Institute KNMI	126	29/35 41/49
42	H.Glaab, B.Fay, I.Jacobsen ***D*** German Weather Service, DWD	106	30/35 42/49
43	F.Bompay ***F*** Meteo-France, Meteo	206	13/14 43/49
44	L.van der Auwera ***B*** Royal Institute of Meteorology of Belgium, KMI	122	32/35 44/49
45	D.P.Griggs ***USA*** Westinghouse Savannah River Laboratory, SPS	132	31/35 45/49
46	D.Schneiter ***CH*** Swiss Meteorological Institute, IMS	130	33/35 46/49
47	* Sci.appl.Intern.Corp. ***USA***	129	34/35 47/49
48, 49	I.Sandu, N.Romanof, V.Cuculeanie, V.Ivanovici, A.Barbu and V.I.Pescaru ***R*** National Institute of Meteorology and Hydrology, NIMH-R	117 212	35/35 48/49 14/14 49/49

Note: The models marked by * have no description (124, 125, 126, 129).

Table 2. Ranking of the models which used ECMWF data

№	Authors, Country, Organization	Models	Ranks
1	H.Glaab, B.Fay, I.Jacobsen ***D*** German Weather Service, DWD	107	1/35 1/49
2	M.Monfort ***F*** French Institute for Nuclear Protection and Safety, IPSN	111	2/35 2/49
3	J.Saltbones, A.Foss, J.Bartnicki ***N*** Norwegian Meteorological Institute, DNMI	131	3/35 7/49
4	H.Yamazawa, M.Chino, H.Nagai, A.Furuno ***J*** Japan Atomic Energy Research Institute JAERI	115	4/35 9/49
5	D.Anfossi ***I*** National Research Council, CNR	114	5/35 5/49
6	J.S.Nasstrom, T.C.Pace ***USA*** Lawrence Livermore Nation. Laboratories, LLNL	127	6/35 12/49
7	A.Stohl ***A*** Institute of Meteorology and Physics, University of Wien, IMP	101	7/35 10/49
8	D.Wendum ***F*** French Electricity EDF	112	8/35 14/49
9	L.Robertson, J.Langner, C.Persson, A.Ullerstig ***S*** Swedish Meteorological and Hydrological Institute, SMHI	128	9/35 15/49
10	T.Iwasaki, T.Maki ***J*** Japan Meteorological Agency, JMA	134	10/35 17/49
11	R.H.Maryon and D.B.Ryall ***UK*** Meteorological Office, Metoff	119	11/35 21/49
12	F.Desiato ***I*** National Agency for Environment, ANPA	113	12/35 18/49
13	L.Thaning ***S*** Defence Research Establishment, FOA	118	13/35 19/49
14	M.Pekar ***RU*** Meteorological Synthesizing Centre East, MSC-E	135	14/35 22/49
15	**** NL*** Royal Dutch Meteorological Institute KNMI	124	15/35 23/49
16	J.Brandt, J.Christensen, A.Ebel, H.Elbern, H.Jacobs, M.Memmesheimer, T.Mikkelsen, S.Thykier-Nielsen and Z.Zlatev ***D/DK*** National Environment Research Institute/Risoe Nat.Lab./Univ.of Cologne, NERI	109	16/35 20/49
17	**** NL*** Royal Dutch Meteorological Institute KNMI	125	17/35 25/49
18	J.Sato, H.Sasaki, K.Adachi ***J*** Meteorological Research Institute, MRI	116	18/35 24/49
19	J.Brandt, J.Christensen, A.Ebel, H.Elbern, H.Jacobs, M.Memmesheimer, T.Mikkelsen, S.Thykier-Nielsen and Z.Zlatev ***D/DK*** National Environment Research Institute/Risoe Nat.Lab./Univ.of Cologne, NERI	108	19/35 28/49
20	R.I.Sykes and R.S.Gabruk ***USA*** ARAP Group of Titan Research and Technology, ARAP	121	20/35 27/49
21	G.O.Hess, R.R.Draxler ***AUS*** Bureau of Meteorological Research Centre, BMRC	102	21/35 30/49
22	J.H.Sørensen, A.Rasmussen ***DK*** Danish Meteorological Institute, DMI	110	22/35 31/49
23	R.D'Amours ***CND*** Canadian Meteorological Centre, CMC	105	23/35 35/49
24	D.Syrakov and M.Prodanova ***BG*** National Institute for Meteorology and Hydrology, NIMH-BG	104	24/35 37/49

25	F.Bompay ***F*** Meteo-France, Meteo	123	25/35 36/49
26	T.Iwasaki, T.Maki ***J*** Japan Meteorological Agency, JMA	133	26/35 40/49

27	B.J.Stunder, B.Draxler, D.Hess ***USA*** National Oceanic and Atmospheric Administration, NOAA	120	27/35 39/49
28	D.Syrakov and M.Prodanova ***BG*** National Institute for Meteorology and Hydrology, NIMH-BG	103	28/35 38/49
29	***** ***NL*** Royal Dutch Meteorological Institute KNMI	126	29/35 41/49
30	H.Glaab, B.Fay, I.Jacobsen ***D*** German Weather Service, DWD	106	30/35 42/49
31	D.P.Griggs ***USA*** Westinghouse Savannah River Laboratory, SPS	132	31/35 45/49
32	L.van der Auwera ***B*** Royal Institute of Meteorology of Belgium, KMI	122	32/35 44/49
33	D.Schneiter ***CH*** Swiss Meteorological Institute, IMS	130	33/35 46/49
34	***** Sci.appl.Intern.Corp. ***USA***	129	34/35 47/49
35	I.Sandu, N.Romanof, V.Cuculeanie, V.Ivanovici, A.Barbu and V.I.Pescaru ***R*** National Institute of Meteorology and Hydrology, NIMH-R	117	35/35 48/49
	Note: The models marked by * have no description (124, 125, 126, 129).		

1. **Model 107.** It is Lagrangian Particle Dispersion Model (LPDM) operating with horizontal resolution $\Delta = 0.5^0$ (55 km). Along the vertical it has 20 layers of which 8 layers are below 1500 m. About 100000 random walk particle trajectories are calculated by Langevin equation.

2. **Model 111.** Semi-Lagrangian Gaussian puff model calculates trajectories and Gaussian puffs from a point source with time step 1 hour. Spatial resolution near the source varies within 0.1^0-2^0. Two puff families of the equal weights are considered at the levels of 1000 mb and 850 mb.

3. **Model 209.** Lagrangian Monte-Carlo model "Name" with spatial resolution Δ = 50 km and 11 layers along the vertical of which 4 layers are below 900 hPa. It operates with UK numerical weather prediction (NWP) model. Skewed turbulent statistics is used for the convective boundary layer. Low-frequency wind meandering and small-scale entrainment and venting by large cumulus are taken into account.

4. **Model 203.** (see variant of model 107) operates with meteorological data of Europe model (EM) - NWP regional model for the North Atlantic and Europe.

5. **Model 114.** It is a Lagrangian particle model MILFORD. Wind speed components are precisely interpolated with time and space. Random fluctuations are determined: $u_i'(t)\Delta t = \sqrt{2K_i \Delta t}\ \mu_i$, where μ_i - random variable with zero mean and variance 1. K_i - horizontal diffusion coefficient, t – time step. The best results are obtained with mixing layer height fixed in time and space (as it was in modelling of Chernobyl accident) and constant diffusion coefficients: $K_x = K_y = 4.5 \times 10^4$ m^2/s, $K_z = 1$ m^2/s.

6. **Model 210.** (see 3, variant of model 209). Another modification of UK NWP is used.

7. **Model 131.** Lagrangian particle model operates with meteorological input data of LAM50S (Limited Area Model 50 km grid resolution). The vertical structure: 14 σ-layers, 7 layers are below 1500 m. Three-dimensional particle velocity is interpolated from 8 nearest knots. Bilinear interpolation in space is applied to velocity horizontal components and linear interpolation - to the vertical component. Diffusion is simulated as random walk in three dimensions.

8. **Model 208.** It is an Eulerian model MATCH in which Lagrangian particle model is used for the determination of initial variance during first 10 hours of transport from the source. Horizontal resolution - 55 km, 16 layers along the vertical. Meteorological model HIRLAM is used.

9. **Model 115.** It is a Lagrangian dispersion model with meteorological preprocessor providing three-dimensional mass-consistent wind fields. It operates with a uniform grid Δ=63.5 km along horizontal and a variable one along the vertical - Δz=100 m in the surface layer up to 900 m in the 20th layer. Atmospheric dispersion is simulated by the motion of a great number of particles (40000) released by a point source. Horizontal diffusion is described by random fluctuations. The mixing layer height is assumed to be constant.

10. **Model 101.** Lagrangian particle dispersion model. All levels of ECMWF data of which nine are below 2800 m are used. Stochastic Langevin equation is solved for particles. Small-scale turbulence in the boundary layer and meso-scale velocity fluctuations are considered. In calculations 10^6 particles are used.

11. **Model 213.** (see 7, model variant 131). In this case operational NWP model HIRLAM is used.

12. **Model 127.** It is a Lagrangian particle model in which advection-diffusion equation is solved by Monte-Carlo method. The vertical layer structure is slightly different from that of ECMWF. 30000 particles are calculated. Beginning with 1600 UTC of each day low-stable conditions and h_{mix} = 400 - 500 m were assumed. At 0800 UTC the conditions are switched on low-unstable ones with h_{mix} = 1000 m.

13. **Model 204.** The model combines Eulerian long-range transport model and Lagrangian mesoscale puff model. Meteorological information of Canadian meteorological centre with spatial resolution 1^0 is used. Heights h_{mix} and K_z were assumed constant over the whole region. Eulerian model has resolution 25 km (in polar stereographic projection). The scheme of finite elements is applied. Horizontal dispersion is determined by constant diffusion coefficient 30000 m^2/s. Lagrangian puff model simulates the release of sequential puffs which are transported and dispersed over the horizontal grid with resolution 5 km.

14. **Model 112.** It is a Lagrangian particle model with application of “kernel distribution method”. The model keeps track of a great number of particles following Eulerian mean flow with random fluctuations simulating turbulence effects. Horizontal diffusion coefficient is K_H=5·10^4 m^2/s.

15. **Model 128.** (see 8, model variant 208). ECMWF meteorological data are used.

16. **Model 205.** Danish three-dimensional model based on multi-level puff parametrization (DERMA). This model uses DMI-HILRAM meteorological data. It is assumed that

species released from the source rapidly fills the boundary layer. Therefore particles are located at equidistant heights from the ground surface up to the top of the boundary layer and they are then transported by three-dimensional wind. Each particle is a puff with dispersion growing with time according to Gifford. Horizontal diffusion coefficient is $5.6 \cdot 10^3$ m^2/s and Lagrangian time-scale $t_L = 10^4$ s.

17. **Model 134.** It operates on the basis of Lagrangian particle method. Horizontal and vertical grids are the same as in ECMWF analysis. Horizontal diffusion was not taken into account. Vertical diffusion is realized by the random walk model. Pollutant dry deposition with velocities 0.17 cm/s over land and 0.77 cm/s over the ocean is calculated.

18. **Model 113.** Long-range Lagrangian particle model APOLLO (Atmospheric POLlutant LOng-range dispersion) designed for the evaluation of concentrations at long distances from the source. The cloud is simulated by a bulk of particles transported by 3-d wind modulated by turbulent pulses. Turbulent motion is calculated by random displacement model.

19. **Model 118.** A particle model with horizontal resolution 63 km and 100 m along the vertical based on the well-known MATHEW/ADPIC models. Mass-consistent wind is used. Particle velocities are determined by mean motion and diffusion velocities. Before standard deviation is less Δx on the subgrid scale, first particles and then Gaussian plume are considered. Near the source nested grid with grid interval Δx=8km is introduced. Calculations are made for mixing layer heights 1000 m and 500 m.

20. **Model 109.** (see 13, model variant 204). Meteorological input data MM5VI with resolution 50 km are used in calculations.

21. **Model 119.** (see 3, model variant 209). A variant of UK meteorological data of operational NWP on the basis of ECMWF data is used.

22. **Model 135.** It is a typical Eulerian model with horizontal resolution 0.25^0 x 0.25^0. It operates with winds and temperature at levels 1000 and 850 mb, surface wind components at 10 m and temperature at 2 m. Numerical advection scheme with conservation of the first three moments of grid concentration element (mass) is used. Horizontal diffusion is calculated by coefficient $K_H = 1.5 \cdot 10^4$ m^2/s. In the vertical direction Monin-Obukhov similarity laws are used.

23. **Model 124.** (KNMI) - the description is not available.

24. **Model 116.** It is a Lagrangian dispersion model with a great number of particles which diffusion is calculated by random walk method. For meteorological fields spline interpolation is applied.

25. **Model 125.** (KNMI) - the description is not available.

26. **Model 211.** Hybrid Single Particle Lagrangian Integrated Trajectory Code (HYSPLIT_4) is used for calculations of trajectories, particles or puff dispersion. The model is based on an unusual approach - along the horizontal puffs are considered, along the vertical - particles. The model operates with the meteorological input from NOAA Aviation model with horizontal resolution ~190 km and 5 levels along the vertical up to 500 hPa. In spite of the fact that AVN data are rougher than those of ECMWF, their application provides better results compared to ECMWF data.

27. **Model 121.** Lagrangian Gaussian puff model. Algorithms of puff splitting and coalescence are used. Changeable time step is used.

28. **Model 108.** (see 13, model variant 204). ECMWF meteorological data with resolution 1.5^0 are used.

29. **Model 214.** (see 22, model variant 135). Data of wind and temperature objective analysis of Russian Hydrometcentre were utilized.

30. **Model 102.** HYSPLIT_4 (Hybrid Single Particle Lagrangian Integrated Trajectory Code, version 4) results with analysed ECMWF meteorological data are presented. The model operates with puffs along the horizontal and particles along the vertical. Advection and diffusion are calculated by Lagrangian approach, concentrations are determined on a fixed grid. Due to diffusion the puff with Gaussian concentration distribution is expanding till it exceeds the grid interval then it is split into several puffs.

31. **Model 102.** (see 16, model variant 205). The model results are obtained with ECMWF meteorological data.

32. **Model 201.** (see 30, model variant 102). In this case meteorological information of Australian Bureau of Meteorology is used.

33. **Model 202.** In ETEX experiment the Canadian Meteorological Centre (CMC) participated with model CANERM (CANadian Emergency Response Model). CANERM is an 3d Eulerian advection-diffusion model with σ - co-ordinates along the vertical, horizontal spatial resolution 25 km and 11 levels with interval $1 < \sigma < 0.5$. Horizontal diffusion is

simulated according to *K* theory. Vertical diffusion is determined by mixing length and Richardson number.

34. Model 207. (see 24, model variant 116).

35. Model 105. (see 33, model variant 202). ECMWF meteorological data are used.

36. Model 123. Eulerian-type 3d model MEDIA is used with ECMWF meteorological input. Horizontal diffusion is calculated by the coefficient dependent on cell size. Vertical diffusion is determined according to Louis. The source is located in the layer within 100 m above the ground surface.

37,38. Models 103, 104. Bulgarian group presented two models in ATMES-II experiment: LED model operating with puff and EMAP -Eulerian multi-level model. Wind and potential temperature at 850 mb and potential temperature on the ground were the only meteorological input for ETEX calculations. LED (Lagrangian-Eulerian Diffusion) is a puff model calculating motion and diffusion of puffs sequentially released by the source. EMAP is Eulerian model for Air Pollution, which employs new advection scheme TRUP. Horizontal diffusion is calculated by an explicit scheme of the second order relative to time, vertical diffusion - by an implicit scheme for variable step along the vertical.

39. Model 120. (see 26, model variant 211). This model uses ECMWF meteorological information.

40. Model 133. (see 17, model variant 134).

41. Model 125. (KNMI) - model description is not available.

42. Model 106. (see 1, model variant 107). In this case a spectral model and ECMWF information are used but with another realization.

43. Model 206. (see 36, model variant 123). French numerical weather prediction model ARPEGE data are used in this model.

44. Model 122. For testing ETEX experiment the Belgium Meteorological Institute used its puff model. Input data - radiosonde observations with time interval 12 hours connected with ECMWF predictions for 00.00 and 12.00 GMT on the surface and at standard levels up to 500 hPa. Resolution: $(\Delta\lambda, \Delta\varphi, \Delta z) = (0.5^0, 0.5^0, \approx 50$ m). The mixing layer height is calculated at each time step in each point by “parcel intersection method”. The boundary layer stability is assessed by parameters of Monin-Obukhov similarity theory. The puff model considers the behavior of sequential Gaussian puffs released from the source and randomly distributed with time. Mass of each puff depends on the release rate and time

of two sequential puffs overlapping. Mass center of puffs is advected by interpolated 3d wind speed. Horizontal diffusion is evaluated according to Gifford, shear diffusion is allowed for. As far as horizontal puff size becomes equal to the grid resolution, the puff is divided into 5 new puffs (one central and 4 symmetrically located to it). The concentration in the surface layer is determined by the input of all puffs below the mixing layer height.

45. **Model 132.** The Savannah River Technology Center (SRTC) provided results of the first ETEX release modelling performed by Colorado State University Regional Atmospheric Modelling System (RAMS) and Lagrangian Dispersion Model (LPDM). RAMS model employs the model output of ECMWF. Horizontal resolution is 75 km, the vertical structure: from 50 m - the first layer to 1250 m - near the model top ~19.7 km AGL.

46. **Model 130.** LORAN (Long Range Atmospheric Advection of Nuclides) model is used. It considers wind at 850 mb surface only. The model considered horizontal extent of the plume and then surface concentrations. The mixing layer height is determined according to *Holstag and van Ulden*. Cross Gaussian expansion is calculated with dispersion variation with time as $\sigma = 0.825\ t$.

47. **Model 129.** The description is not available.

48,49. **Models 117, 212.** The results are obtained by Romanian Lagrangian Puff Model (RLPM) with ECMWF meteorological data and meteorological data provided by the Romanian weather prediction model LMD5. The airborne transport is realized by a great number of puffs released from a point source. The result of advection is trajectories of puffs, which were calculated with mean wind velocity. The formula for Gaussian concentration distribution makes the basis for calculating concentrations from all puffs and for solving the problem considered.

Discussion of the results

Ranking of the models is presented in tables 1,2. Tables 3,4 demonstrate ranking of models including methods they used. The main result lies in the fact that models based on Lagrangian particle method predominate. Among the first 15 models of table 3 only three models use other approaches: the model of M.Monfort which has rank 2 uses semi-Lagrangian Gaussian puff-method; the model of *L.Robertson, J.Langner, C.Persson, A.Ullerstig* which combines Lagrangian method with particles for 10 hours of transport from the source and Eulerian approach after 10 hours. This model has rank 8. Model 204 of a

group of authors: *J.Brandt, J.Christensen, A.Ebel, H.Elbern, H.Jacobs*, *M.Memmesheimer, T.Mikkelsen, S.Thykier-Nielsen and Z.Zlatev* has rank 13 which is based on Lagrangian particle method near the source and then Eulerian method over the whole grid is used. Actually this and the previous models can be attributed to the whole group of 15 models. It is necessary to stress that particles approach requires a lot of calculations and memory (for example, 100000 random trajectories are calculated by model 1).

Then come models based on puff methods (as a rule Gaussian), puff+ Eulerian continuation, purely Eulerian approach, particles+puffs, particles along the vertical, puffs - in horizontal. In our view in this case the predominant method cannot be distinguished: the mentioned above approaches participate actually with the same frequency in the interval from 16 to 49 models. The list of models based on purely Eulerian approach begins with MSC-E model and they are 7 all together.

Table 4 demonstrates a similar ranking of 35 models operating with ECMWF meteorological information. The predomination of the particle method, which occupies the first ranks is evident. Among other methods it is impossible to give preference to a single one.

As a result of model comparison the following conclusions could be made:

Best results in the transport evaluation near the point source were achieved by group of Lagrangian particle models.

EMEP/MSC-E 3-D Eulerian model participated in the evaluation of transport from point sources gave reasonable results in comparison with different types of models. In ATMES the MSC-E/EMEP model demonstrated the fourth results in regard to the calculations: Cs^{137} concentration, I^{131} concentration, Cs^{137} deposition. In ATMES-II MSC-E has the following results: for model 135 (with meteorological data of ECMWF) 14/35, 22/49, for model 214 (meteorological data of Hydrometeorological Centre of Russia) 9/14, 29/49.

Combination of Lagrangian particle method for point source with Eulerian one for the whole EMEP region could improve quality of long-range transport modelling.

In model development a special attention is given to Chaos theory, Mixing theory, application of data assimilation to emergency response, etc.

References

Mosca S., R.Bianconi, R.Bellasio, G.Grasiani and W. Klug [1998] ATMES-II - Evaluation of long-range dispersion models using data of the 1st ETEX release. Luxembourg: Office of Official Publications of the European Communities, 1998.

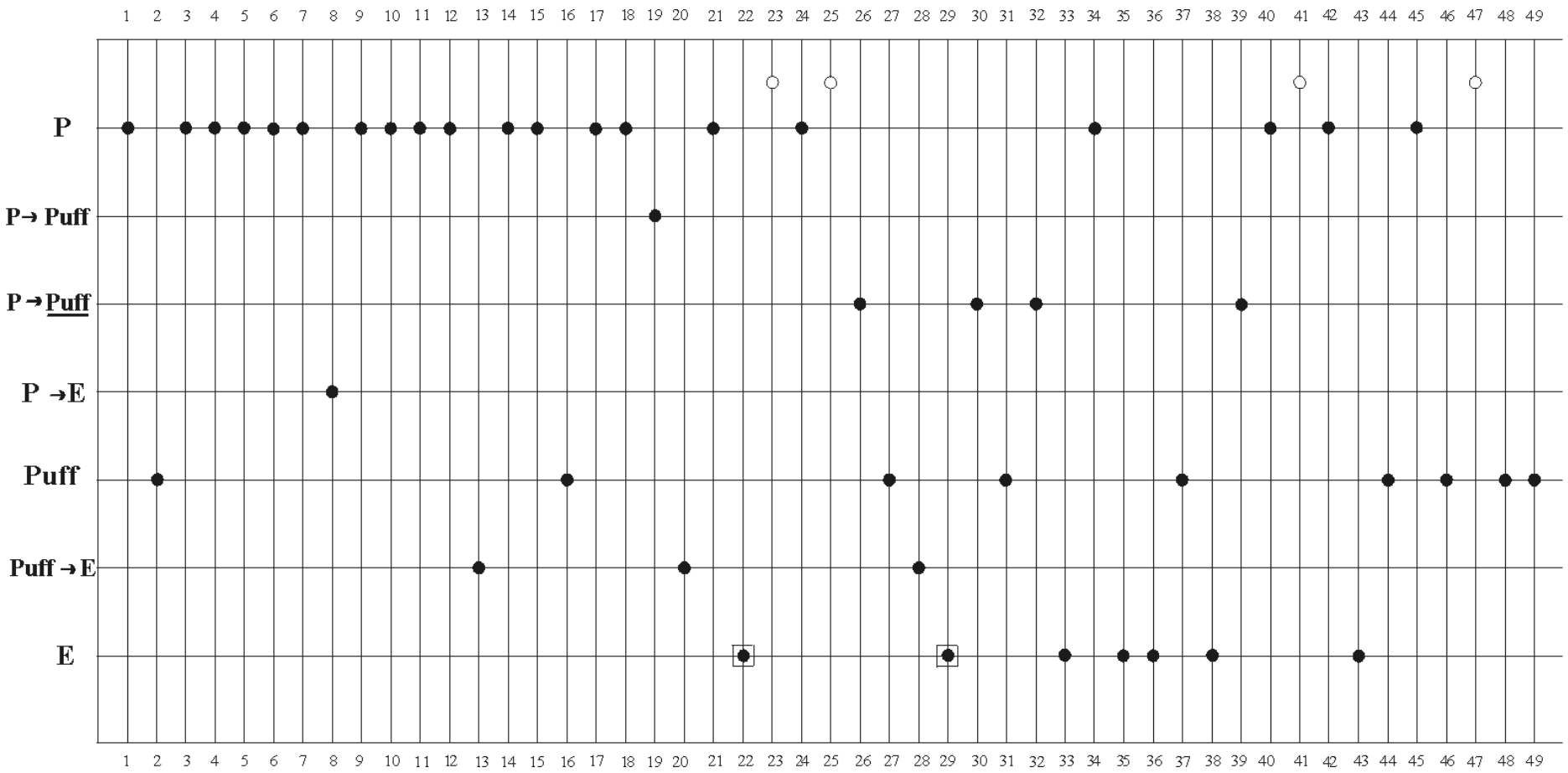

Table 3. Ranking of models participated in ATMES-II according to their modelling approach

Modelling approach: **P** - particles; **P** → **Puff** - particles-puff; **P** → **Puff** -particles along the vertical, puff - along the horizontal; **P** → **E** - particles-Eulerian approach; **Puff** - puffs, **Puff** → **E** - puffs - Eulerian approach; **E** - Eulerian approach.

Empty circles - models without description.

2 models marked by squares - MSC-E models.

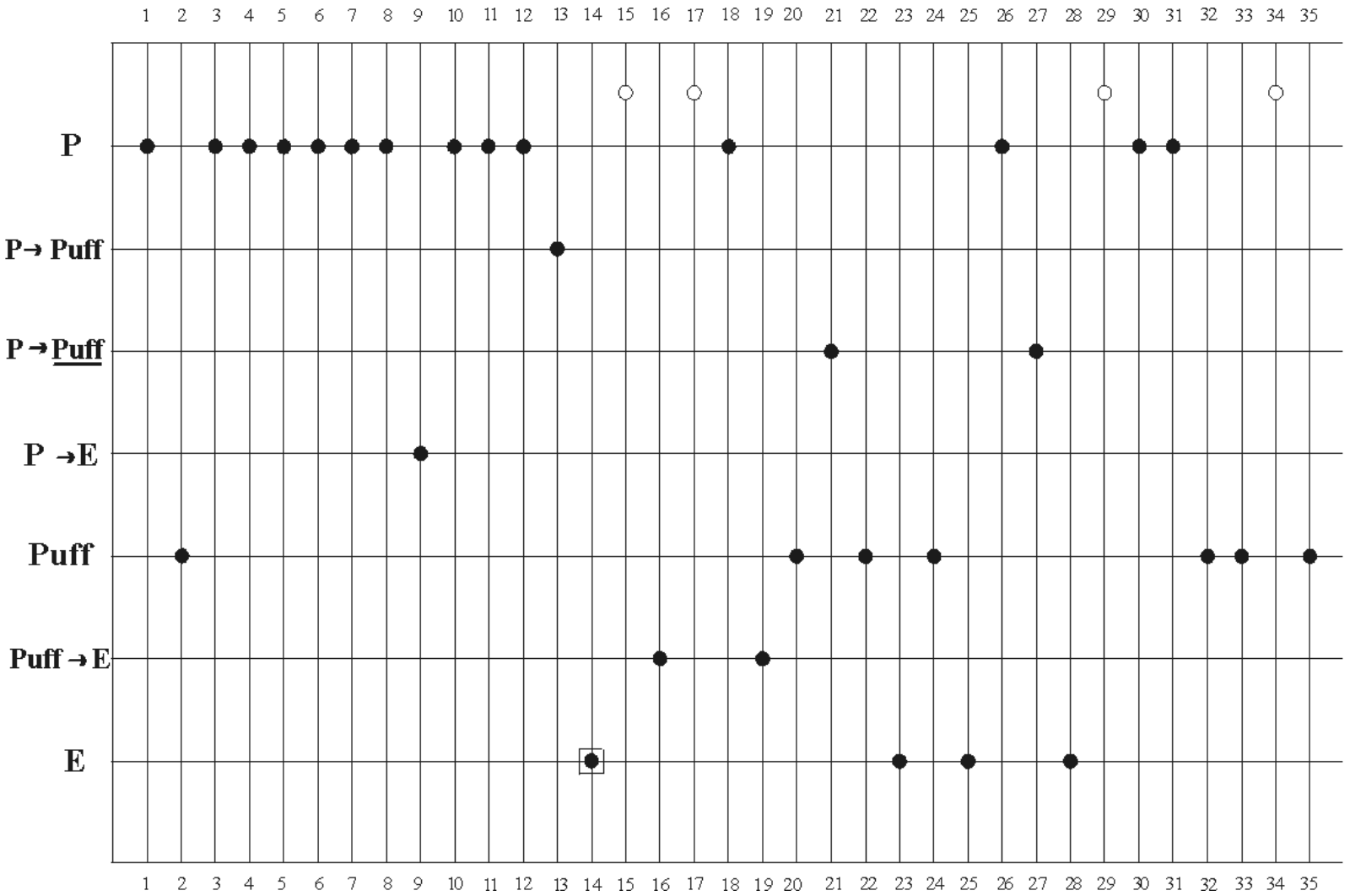

Table 4. Order of models which used ECMWF meteorological data according to their ranks and modelling approach

Modelling approach: **P** - particles; **P** → **Puff** - particles-puff; **P** → **Puff** -particles along the vertical, puff - along the horizontal; **P** → **E** - particles-Eulerian approach; **Puff** - puffs, **Puff** → **E** - puffs - Eulerian approach; **E** - Eulerian approach.

Empty circles - models without description.

Model marked by squares - MSC-E model